



# Synergy between Interleukin-1 $\beta$ , Interferon- $\gamma$ , and Glucocorticoids to Induce TLR2 Expression Involves NF- $\kappa$ B, STAT1, and the Glucocorticoid Receptor<sup>SI</sup>

Akanksha Bansal, Cora Kooi, Keerthana Kalyanaraman, Sachman Gill, Andrew Thorne, Priyanka Chandramohan, Amandah Necker-Brown,  Mahmoud M. Mostafa, Arya Milani, Richard Leigh, and  Robert Newton

Departments of Physiology and Pharmacology (A.B., K.K., S.G., A.T., P.C., A.N.-B., M.M.M., A.M., R.N.) and Medicine (C.K., R.L.), Lung Health Research Group, Snyder Institute for Chronic Diseases, Cumming School of Medicine, University of Calgary, Alberta, Canada

Received June 18, 2023; accepted September 29, 2023

## ABSTRACT

Glucocorticoids act via the glucocorticoid receptor (GR; NR3C1) to downregulate inflammatory gene expression and are effective treatments for mild to moderate asthma. However, in severe asthma and virus-induced exacerbations, glucocorticoid therapies are less efficacious, possibly due to reduced responsiveness and/or the increased expression of proinflammatory genes. In human A549 epithelial and primary human bronchial epithelial cells, toll-like receptor (TLR)-2 mRNA and protein were *supra*-additively induced by interleukin-1 $\beta$  (IL-1 $\beta$ ) plus dexamethasone (IL-1 $\beta$ +Dex), interferon- $\gamma$  (IFN- $\gamma$ ) plus dexamethasone (IFN- $\gamma$ +Dex), and IL-1 $\beta$  plus IFN- $\gamma$  plus dexamethasone (IL-1 $\beta$ +IFN- $\gamma$ +Dex). Indeed, ~34- to 2100-fold increases were apparent at 24 hours for IL-1 $\beta$ +IFN- $\gamma$ +Dex, and this was greater than for any single or dual treatment. Using the A549 cell model, TLR2 induction by IL-1 $\beta$ +IFN- $\gamma$ +Dex was antagonized by Org34517, a competitive GR antagonist. Further, when combined with IL-1 $\beta$ , IFN- $\gamma$ , or IL-1 $\beta$ +IFN- $\gamma$ , the enhancements by dexamethasone on TLR2 expression required GR. Likewise, inhibitor of  $\kappa$ B kinase 2 inhibitors reduced IL-1 $\beta$ +IFN- $\gamma$ +Dex-induced TLR2 expression, and TLR2 expression induced by IL-1 $\beta$ +Dex, with or without IFN- $\gamma$ , required the nuclear factor (NF)- $\kappa$ B subunit, p65. Similarly, signal transducer and activator of transcription (STAT)-1 phosphorylation and  $\gamma$ -interferon-

activated sequence-dependent transcription were induced by IFN- $\gamma$ . These, along with IL-1 $\beta$ +IFN- $\gamma$ +Dex-induced TLR2 expression, were inhibited by Janus kinase (JAK) inhibitors. As IL-1 $\beta$ +IFN- $\gamma$ +Dex-induced TLR2 expression also required STAT1, this study reveals cooperation between JAK-STAT1, NF- $\kappa$ B, and GR to upregulate TLR2 expression. Since TLR2 agonism elicits inflammatory responses, we propose that synergies involving TLR2 may occur within the cytokine milieu present in the immunopathology of glucocorticoid-resistant disease, and this could promote glucocorticoid resistance.

## SIGNIFICANCE STATEMENT

This study highlights that in human pulmonary epithelial cells, glucocorticoids, when combined with the inflammatory cytokines interleukin-1 $\beta$  (IL-1 $\beta$ ) and interferon- $\gamma$  (IFN- $\gamma$ ), can synergistically induce the expression of inflammatory genes, such as TLR2. This effect involved positive combinatorial interactions between NF- $\kappa$ B/p65, glucocorticoid receptor, and JAK-STAT1 signaling to synergistically upregulate TLR2 expression. Thus, synergies involving glucocorticoid enhancement of TLR2 expression may occur in the immunopathology of glucocorticoid-resistant inflammatory diseases, including severe asthma.

## Introduction

Synthetic glucocorticoids, administered as inhaled corticosteroids (ICS), are widely and successfully used to treat mild to moderate asthma (Rhen and Cidlowski, 2005). However, in patients with severe neutrophilic (a.k.a. T2 low) asthma

or viral exacerbations or those who smoke or have chronic obstructive pulmonary disease, ICS medications exhibit reduced clinical efficacy (Barnes, 2013). Thus, partial, or complete, unresponsiveness to ICS therapy in such conditions is often referred to as glucocorticoid resistance or insensitivity. Furthermore, the elevation of ICS dose and/or the inclusion of oral glucocorticoids with the aim of achieving increased clinical effectiveness in such patients leads to systemic adverse effects that include reduced hypothalamus-pituitary-adrenal axis function, weight gain, osteoporosis, hypertension, and hyperglycemia leading to diabetes (Liu et al., 2013).

Glucocorticoids act on the glucocorticoid receptor (GR; NR3C1) to suppress the expression of inflammatory mediators and thereby attenuate inflammation (Rhen and Cidlowski, 2005; Newton and Holden, 2007). These effects of glucocorticoid

This work was supported by grants from the Canadian Institutes of Health Research (CIHR) [funding reference numbers: PJT 156310 (to R.N.) and 180480 (to R.N. and R.L.)] and a Natural Sciences and Engineering Research Council of Canada (NSERC) discovery [Grant RGPIN-2016-04549] (to R.N.); studentships (to A.B.): Eyes High Doctoral Scholarship and Eleanor Mackie Doctoral Scholarship in Women's Health from University of Calgary. The funding bodies played no role in the design of the study and collection, analysis, and interpretation of data.

No author has an actual or perceived conflict of interest with the contents of this article.

dx.doi.org/10.1124/molpharm.123.000740.

<sup>SI</sup> This article has supplemental material available at [molpharm.aspetjournals.org](http://molpharm.aspetjournals.org).

on airway epithelial cells are also thought to be essential in the resolution of lung inflammation caused by allergen inhalation (Klaßen et al., 2017). Glucocorticoids diffuse through the cell membrane and bind to cytoplasmic GR to drive its nuclear translocation. In the nucleus, ligand-bound GR acts as a transcription factor by binding to palindromic glucocorticoid response elements (GREs), which are located in the regulatory regions of target genes. These DNA elements are responsible for driving glucocorticoid-induced expression of many metabolic and anti-inflammatory genes (Jantzen et al., 1987; Imai et al., 1990; Newton and Holden, 2007). However, ligand-activated GR may also interact with inflammatory transcription factors, such as nuclear factor  $\kappa$ B (NF- $\kappa$ B) and AP-1, and this effect is often suggested as directly causing transcriptional repression (De Bosscher and Haegeman, 2009). Despite this, an increasing body of evidence clearly shows that GR can positively interact with inflammatory transcription factors, resulting in additive, or even synergistic, transcriptional outcomes (Hofmann and Schmitz, 2002; Altonsy et al., 2014; Miyata et al., 2015; Newton et al., 2017; Oh et al., 2017). Thus, glucocorticoid-activated mechanisms variously increase or decrease the expression of inflammatory genes. As a consequence, glucocorticoids should more accurately be considered as being immunomodulatory rather than simply being “anti-inflammatory” (Busillo and Cidlowski, 2013; Cruz-Topete and Cidlowski, 2015; Newton et al., 2017; Amrani et al., 2020).

Aside from being a primary target for therapy, the airway epithelium is first in line to encounter inhaled particulate matter and microbes that enter the airways (Tam et al., 2011; Lambrecht and Hammad, 2012). Although these structural cells serve as a physical barrier, they are also fundamental in shaping inflammatory responses (Tam et al., 2011; Lambrecht and Hammad, 2012). In response to environmental insults and stimuli, airway epithelial cells release proinflammatory cytokines, chemokines, and inflammatory enzymes via activation of inflammatory signaling pathways (Lambrecht and Hammad, 2012). Cytokines, such as interleukin-1 $\beta$  (IL-1 $\beta$ ) and tumor necrosis factor (TNF)- $\alpha$  are central to inflammatory responses, to a large extent due to the activation of the I $\kappa$ B kinase (IKK)-NF- $\kappa$ B pathway (Pahl, 1999). Similarly, interferon- $\gamma$  (IFN- $\gamma$ ) activates Janus kinase (JAK)-signal transducer and activator of transcription (STAT) signaling and is a key regulator of immune responses related to viral infection and humoral immunity (Schroder et al., 2004). Interactions between IFN- $\gamma$ - and TNF-mediated pathways are also implicated in promoting glucocorticoid resistance (Tliba et al., 2008; Britt et al., 2019). Furthermore, IL-1 $\beta$  and IFN- $\gamma$  play a variety of roles in airway inflammatory responses, including in severe asthma and both bacterial and viral exacerbations of asthma (Ngoc et al., 2005; Lambrecht et al., 2019). Since glucocorticoids are

frequently employed as a treatment in these conditions, albeit with reduced efficacy, the coregulation of inflammatory genes by glucocorticoids IL-1 $\beta$  and IFN- $\gamma$  is likely to be important to the mechanisms that underlie glucocorticoid insensitivity.

Toll-like receptor (TLR)-2 is located on the surface of airway epithelial cells and recognizes pathogen-associated molecular patterns present in many bacteria, viruses, and other microbes (Akira et al., 2001). In a prior study (Bansal et al., 2022), we investigated the synergistic induction of TLR2 expression in airway epithelial cells by glucocorticoids and proinflammatory cytokines (IL-1 $\beta$  and TNF), which involved positive cooperativity between GR and NF- $\kappa$ B. However, although studies also suggest that glucocorticoids enhance TLR2 expression induced by combinations of TNF and IFN- $\gamma$  (Homma et al., 2004; Winder et al., 2009), molecular mechanisms underlying such effects are not established. As many biologic effects of IFN- $\gamma$  are manifested via the transcription factor STAT1 (Schroder et al., 2004), we interrogated possible roles and interactions between GR, NF- $\kappa$ B and STAT1 in the regulation of TLR2 expression.

## Materials and Methods

**Stimuli, Drugs, and Other Inhibitors.** Recombinant human IL-1 $\beta$  (R&D Systems) was dissolved in PBS containing 0.1% bovine serum albumin (Sigma-Aldrich). Recombinant human IFN- $\gamma$  (R&D Systems) was dissolved in deionized sterile water. Budesonide (gift from AstraZeneca, Sweden), dexamethasone (Dex; Sigma-Aldrich), Organon 34517 (Org34517) (gift from Chiesi Farmaceutici, Parma, Italy), N-(6-chloro-9h-pyrido[3,4-b]indol-8-yl)-3-pyridinecarboxamide (PS-1145) (Sigma-Aldrich), N-(6-Chloro-7-methoxy-9H-pyrido[3,4-b]indol-8-yl)-2-methyl-3-pyridinecarboxamide dihydrochloride (ML120B) (SML1174, Sigma-Aldrich), 2-[(Aminocarbonyl)amino]-5-(4-fluorophenyl)-3-thiophenecarboxamide (TPCA-1) (2559, Tocris), (S)-5-chloro-N2-(1-(5-fluoropyrimidin-2-yl)ethyl)-N4-(5-methyl-1H-pyrazol-3-yl)pyrimidine-2,4-diamine (AZD1480) (5617, Tocris),  $\beta$ R-cyclopentyl-4-(7H-pyrrolo[2,3-day]pyrimidin-4-yl)-1H-pyrazole-1-propanenitrile (ruxolitinib) (7067, Tocris), and 3-Azetidineacetoneitrile, 1-(ethylsulfonyl)-3-[4-(7H-pyrrolo[2,3-day]pyrimidin-4-yl)-1H-pyrazol-1-yl]- (baricitinib) (7222, Tocris) were dissolved in DMSO as stocks of 10 mM. Final DMSO concentrations on cells were  $\leq$ 0.1%. G418 (A1720, Sigma-Aldrich) was dissolved in sterile water as stocks of 100 mg/ml.

**Submersion Culture of Cells.** A549 human pulmonary type II epithelial cells (American Type Culture Collection CCL-185; Research Resource Identifier: CVC\_0023L) were cultured in Dulbecco's modified Eagle's medium supplemented with 10% FBS and 2 mM L-glutamine (all Thermo Fisher Scientific). Nontransplanted normal human lungs obtained from the tissue retrieval service at the International Institute for the Advancement of Medicine (Edison, NJ) were used to isolate primary human bronchial epithelial cells (pHBECs) as previously described (Hudy et al., 2010). No personal identifying information was provided, and local ethics approval was granted via the Conjoint Health Research Ethics Board of the

**ABBREVIATIONS:** ALI, air-liquid interface; AZD1480, (S)-5-chloro-N2-(1-(5-fluoropyrimidin-2-yl)ethyl)-N4-(5-methyl-1H-pyrazol-3-yl)pyrimidine-2, 4-diamine; baricitinib, 3-Azetidineacetoneitrile, 1-(ethylsulfonyl)-3-[4-(7H-pyrrolo[2, 3-day]pyrimidin-4-yl)-1H-pyrazol-1-yl]-; Bud, budesonide; Dex, dexamethasone; GAS,  $\gamma$ -interferon-activated sequence; GR, glucocorticoid receptor; GRE, glucocorticoid response element; ICS, inhaled corticosteroid; IFN- $\gamma$ , interferon- $\gamma$ ; IFN- $\gamma$ +Dex, IFN- $\gamma$  plus dexamethasone; IKK, I $\kappa$ B kinase; IL-1 $\beta$ , interleukin-1 $\beta$ ; IL-1 $\beta$ +Bud, IL-1 $\beta$  plus budesonide; IL-1 $\beta$ +Dex, IL-1 $\beta$  plus dexamethasone; IL-1 $\beta$ +IFN- $\gamma$ +Bud, IL-1 $\beta$  plus IFN- $\gamma$  plus budesonide; IL-1 $\beta$ +IFN- $\gamma$ +Dex, IL-1 $\beta$  plus IFN- $\gamma$  plus dexamethasone; JAK, Janus kinase; MAPK, mitogen activated protein kinase; ML120B, N-(6-Chloro-7-methoxy-9H-pyrido[3, 4-b]indol-8-yl)-2-methyl-3-pyridinecarboxamide dihydrochloride; MTT, 3-[4, 5-Dimethylthiazol-2-yl]-2, 5-diphenyltetrazolium bromide; NF- $\kappa$ B, nuclear factor  $\kappa$ B; Org34517, Organon 34517; pHBEC, primary human bronchial epithelial cell; PS-1145, N-(6-chloro-9h-pyrido[3, 4-b]indol-8-yl)-3-pyridinecarboxamide; ruxolitinib,  $\beta$ R-cyclopentyl-4-(7H-pyrrolo[2, 3-day]pyrimidin-4-yl)-1H-pyrazole-1-propanenitrile; siRNA, short interfering RNA; STAT, signal transducer and activator of transcription; TLR, toll-like receptor; TNF, tumor necrosis factor; TPCA-1, 2-[(Aminocarbonyl)amino]-5-(4-fluorophenyl)-3-thiophenecarboxamide.

University of Calgary (Study ID: REB15-0336). Cells were grown at 37°C in 5% CO<sub>2</sub>:95% air as submersion cultures using complete airway epithelial cell medium (PromoCell). To arrest growth and reducing activation of pathways, cells were incubated in serum- and additive-free basal media overnight prior to all experiments. A549 cells were periodically checked for possible mycoplasma contamination and tested negative. pHBECS were not tested for mycoplasma contamination.

**Air-Liquid Interface Culture of pHBECS.** pHBECS were grown in air-liquid interface (ALI) culture using transwell inserts (3408, Corning) as previously described (Warner et al., 2019; Michi and Proud, 2021). Over 5 to 6 weeks, this method produces a highly differentiated cell layer that is made up of mucus-producing goblet cells, ciliated columnar epithelial, and basal cells that very closely resemble a normal airways epithelium (Michi and Proud, 2021). Details of our ALI methodology were recently published (Bansal et al., 2022). Only highly differentiated ALI cultures were used. Prior to experiments, cells were fed basally with PneumaCult-ALI basal media (05002, StemCell), with no supplements for 18 hours. The cells were then washed with PBS to remove excess mucus prior to both apical and basolateral application of drugs and/or stimuli in fresh medium. Apical treatments (200  $\mu$ l/well) were diluted in 0.025 M HEPES in F12 and removed after 6 hours, whereas basolateral treatments (1 ml/well) were in PneumaCult-ALI basal medium.

**RNA Extraction, cDNA Synthesis, and Quantitative Polymerase Chain Reaction.** Total RNA was extracted, and 500 ng was used for cDNA synthesis as described (Bansal et al., 2022). cDNA was diluted 1:5 prior to using 2.5  $\mu$ l for polymerase chain reaction (StepOnePlus, Applied Biosciences or QuantStudio3, Thermo Fisher Scientific) with Fast SYBR Green Master Mix (4385618, Thermo Fisher Scientific) and primers specific for TLR2 (forward: GCT GCT CGG CGT TCT CTC and reverse: AAG CAG TGA AAG AGC AAT GGG) and GAPDH (forward: TTC ACC ACC ATG GAG AAG GC and reverse: AGG AGG CAT TGC TGA TGA TCT) as described (Bansal et al., 2022). Relative cDNA concentrations were obtained using standard curves generated by serial dilution of a stimulated cDNA sample analyzed alongside experimental samples. Amplification conditions were 95°C for 20 seconds, then 40 cycles of 95°C for 3 seconds and 60°C for 30 seconds. Primer specificity was assessed by melt curve analysis using 95°C for 3 seconds and 60°C for 30 seconds followed by ramping to 95°C at 0.1°C/s with continuous fluorescent measurement. A single peak in the change of fluorescence with temperature was indicative of primer specificity.

**Western Blotting.** Western blotting was carried out using standard methods (King et al., 2009). Following cell lysis, proteins were size-fractionated in SDS-PAGE gels prior to transferring to nitrocellulose membranes. After blocking, membranes were probed with primary antibodies against TLR2 (12276, Cell Signaling; RRID: AB\_2797867 and ab108998, Abcam; RRID: AB\_10861644), I $\kappa$ B $\alpha$  (sc-371, SantaCruz; RRID: AB\_10861644), Ser32/Ser36 phosphorylated I $\kappa$ B $\alpha$  (9246, Cell Signaling; RRID: AB\_2267145), p65 (sc-8008, Santa-Cruz RRID: AB\_628017), Ser536 phosphorylated p65 (3036, Cell Signaling; RRID: AB\_331281), GR (PA1-511A, Thermo Fisher Scientific; RRID: AB\_2236340), Tyr701 phosphorylated STAT1 (9167, Cell Signaling; RRID: AB\_561284), Ser727 phosphorylated STAT1 (9177, Cell Signaling; RRID: AB\_2197983), STAT1 (9172, Cell Signaling; RRID: AB\_2198300), or GAPDH (MCA4739, Bio-Rad; RRID: AB\_1720065). Following overnight incubation at 4°C, the membranes were washed in Tris-buffered saline with 0.05% v/v Tween 20 detergent and incubated, as appropriate, with 1:5000 or 1:10,000 dilutions of rabbit or mouse horseradish peroxidase-conjugated secondary immunoglobulin (Jackson ImmunoResearch) at room temperature. Immune complexes were detected by enhanced chemiluminescence (Bio-Rad), and images were captured using a ChemiDoc Touch imaging system (Bio-Rad). Densitometric analysis was performed using ImageLab software (Bio-Rad). Note: TLR2

western blots shown in Fig. 1A were generated using ab108998 (Abcam); all other TLR2 blots were generated using 12276 (Cell Signaling) due to the discontinuation of ab108998.

**siRNA-Mediated Knockdown.** Pools of four nontargeting short interfering RNAs (siRNAs) (SI03650325, SI03650318, SI04380467, 1022064), GR siRNAs (SI00003745, SI02654757, SI00003766, SI02654764), RELA siRNAs (SI02663101, SI05146204, SI00301672, SI02663094), and STAT1 siRNAs (SI03119025, SI04950960, SI02662884, SI05078556) (all from Qiagen) were mixed with 3  $\mu$ l Lipofectamine RNAiMax (13778150, Thermo Fisher Scientific) in 100  $\mu$ l Opti-MEM (31985070, Thermo Fisher Scientific) before incubation at room temperature for 5 minutes. This mixture was then added to A549 cells, at approximately 70% confluency, in serum-containing growth medium and incubated for 24–48 hours until the cells were confluent.

**Luciferase Reporter Constructs and Assay.** A549 cells containing the NF- $\kappa$ B reporter 6 $\kappa$ Btk.luc and the GRE reporter 2 $\times$ GRE.luc are previously described (Newton et al., 1998; Chivers et al., 2004). To generate the 3 $\times$ STAT1.luc reporter, oligonucleotides containing three tandem repeats of a consensus STAT1 motif (JASPAR database), also known as a  $\gamma$ -interferon-activated sequence (GAS) (Decker et al., 1997), were designed to generate flanking *KpnI* and *XhoI* sticky ends. These oligonucleotides were annealed by heating to 95°C for 5 minutes prior to cooling to room temperature over a 45-minute period in 10 mM Tris (pH 7.5), 50 mM NaCl, and 1 mM EDTA. Annealed STAT1 oligonucleotides were cloned into *KpnI* (R3142, New England Biolabs) and *XhoI* (R0146, New England Biolabs) digested pGL3.TATA.neo vector (Catley et al., 2004) to generate pGL3.3 $\times$ STAT1.TATA.neo. Twelve micrograms of each reporter, or empty vector (as control), was transfected into subconfluent A549 cells in T-75 flasks using Lipofectamine 2000 (11668019, Thermo Fisher Scientific) 24 hours prior to addition of 1 mg/ml G418 (Sigma-Aldrich). After 14–21 days, foci of G418-resistant cells were passaged in the presence of G418 (0.5 mg/ml) prior to cryo-storage. Luciferase assays were performed using the Firefly Luciferase Assay Kit 2.0 (30085, Biotium Inc.), and luminescence was measured in a 20/20n luminometer (Promega).

**3-(4,5-Dimethylthiazol-2-yl)-2,5-Diphenyltetrazolium Bromide Assay.** Cell viability was measured using a 3-(4,5-Dimethylthiazol-2-yl)-2,5-diphenyltetrazolium bromide (MTT) Assay. MTT (#298-93-1, Sigma-Aldrich) was dissolved in Hank's balanced salt solution (14170112, Thermo Fisher Scientific) to achieve a concentration of 1 mg/mL. Cells grown in 24-well plates were pretreated with IKK2 inhibitors 90 minutes prior to being treated with IL-1 $\beta$  (1 ng/mL). After 6 hours, supernatants were removed, and 100  $\mu$ L of MTT solution was added to each well. After 10–20 minutes of incubation in 37°C in 5% CO<sub>2</sub>/95% air, MTT solution was removed, and 200  $\mu$ L of DMSO was added. The solution was transferred to a 96-well plate, and absorbance was measured at 570 nm.

**Data Presentation and Statistical Analysis.** Data were assumed to be normally distributed and are generally presented as means  $\pm$  S.D. with scatterplots to show individual data points. Multiple comparisons between groups of normally distributed data were made using one-way ANOVA with the appropriate post hoc test (Tukey's or Dunnett's) as indicated. Comparisons between two treatment groups were made using two-tailed, paired Student *t* tests. The number of independent experiments (*N*) is indicated in each graph, and sample sizes (*N*) for experiments were not prespecified. To test for greater than simple additivity, the sum of the effects (i.e., fold – 1) of each treatment (IL-1 $\beta$ , IFN- $\gamma$ , or glucocorticoid alone) (sum) was compared with the effect of cotreatment (comb). GraphPad Prism software (version 6.01 and 10; Dotmatics, Boston, MA) was used for statistical analyses and graph plotting. All analyses in the current study were exploratory and were not designed to test prespecified statistical null hypotheses. Consequently, all calculated *P* values are descriptive and should not be viewed as hypothesis testing.

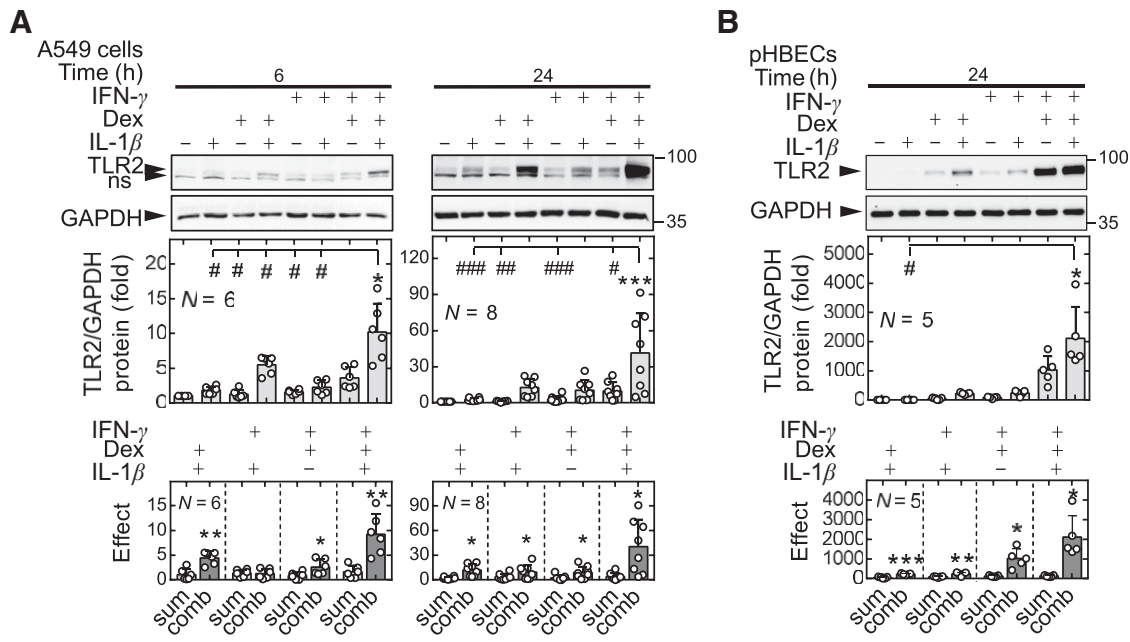


**Fig. 1.** Combinatorial effect of IL-1 $\beta$ , IFN- $\gamma$ , and glucocorticoid on TLR2 protein expression in pulmonary epithelial cells. (A) A549 cells or (B) pHBECs grown in submersion culture were either not treated or treated with IL-1 $\beta$  (1 ng/ml), IFN- $\gamma$  (10 ng/ml), and/or Dex (1  $\mu$ M) as indicated. Cells were harvested at 6 or 24 hours for western blot analysis of TLR2 and GAPDH. Representative blots from  $N$  independent experiments are shown. (Upper graphs) Densitometric data were normalized to GAPDH, expressed as fold of untreated, and mean  $\pm$  S.D. were plotted as bar graphs with overlaid scatter plots. Significance was tested using ANOVA with a Tukey post hoc test. Asterisks (\*, \*\*, or \*\*\*) represent significance relative to untreated. Hash (#, ##, or ###) represent significance relative to IL-1 $\beta$ +IFN- $\gamma$ +Dex. (Lower graphs) The sum of each effect (i.e., fold - 1) within a group of treatments (sum) and the effect (fold - 1) for each combination treatment (comb) is expressed as mean  $\pm$  S.D. and plotted as bar graphs overlaid with scatter plots. Significance was tested by paired  $t$  test. \*,  $P \leq 0.05$ ; \*\*,  $##P \leq 0.01$ ; \*\*\*,  $###P \leq 0.001$ . ns, nonspecific band.

## Results

### Regulation of TLR2 Protein Expression by IL-1 $\beta$ , IFN- $\gamma$ , and Glucocorticoid in Pulmonary Epithelial Cells.

In previous studies, IL-1 $\beta$ , at 1 ng/ml, produced maximal, or near maximal, NF- $\kappa$ B DNA-binding activity as well as NF- $\kappa$ B-dependent reporter activity and cytokine release in A549 cells (Newton et al., 1996; Catley et al., 2004). Similarly, dexamethasone, at 1  $\mu$ M, and budesonide (Bud), a clinically relevant glucocorticoid, at 300 nM, elicited maximal activation of simple GRE-dependent transcription and maximal expression of glucocorticoid-induced genes (Kelly et al., 2012; Rider et al., 2015). Since dexamethasone and budesonide produced near identical expression profiles in A549 cells (Mostafa et al., 2019), dexamethasone was used as the representative glucocorticoid in the A549 cells and pHBECs grown in submersion cultures, whereas budesonide was used in pHBECs grown at ALI.

In A549 cells, IL-1 $\beta$  at 1 ng/ml and dexamethasone at 1  $\mu$ M each very modestly induced TLR2 protein at 6 hours, with slightly increased effects observed at 24 hours (Fig. 1A, upper panels). These effects were enhanced by IL-1 $\beta$  plus dexamethasone (IL-1 $\beta$ +Dex) such that the combination effect of IL-1 $\beta$ +Dex (i.e., fold IL-1 $\beta$ +Dex - 1) (comb) was greater ( $P \leq 0.01$ ) than the summation (sum) of the effects of IL-1 $\beta$  and dexamethasone (i.e., fold IL-1 $\beta$ -1 + fold dexamethasone-1) (Fig. 1A, lower panels). Since these data are consistent with our prior report in which IL-1 $\beta$ +Dex-induced TLR2 mRNA expression was maximal at 6 hours, and greater TLR2 protein expression was apparent at 24 hours (Bansal et al., 2022), these times were also used to investigate the

additional effect of IFN- $\gamma$  on IL-1 $\beta$ +Dex-induced TLR2. Although IFN- $\gamma$  (10 ng/ml), at a concentration that induces chemokine release in epithelial cells (Tudhope et al., 2007), produced very little effect at 6 hours, cotreatment with IL-1 $\beta$  produced a modest increase in TLR2 protein expression. However, cotreatment of IFN- $\gamma$  plus dexamethasone (IFN- $\gamma$ +Dex) increased TLR2 protein expression in a manner that was greater ( $P \leq 0.05$ ) than simple additivity (Fig. 1A). Thus, by 24 hours, IFN- $\gamma$ +Dex increased TLR2 protein levels by 10.7-fold and again revealed *supra*-additivity ( $P \leq 0.05$ ). Upon combined stimulation with IL-1 $\beta$  plus IFN- $\gamma$  plus dexamethasone (IL-1 $\beta$ +IFN- $\gamma$ +Dex), TLR2 protein was increased ( $P \leq 0.05$ ) to 11.3-fold at 6 hours, and this was further increased to 33.6-fold ( $P \leq 0.05$ ) by 24 hours (Fig. 1A). In each case, this response was markedly ( $P \leq 0.05$ ) more than each individual treatment, and, at 24 hours, TLR2 protein expression induced by IL-1 $\beta$ +IFN- $\gamma$ +Dex was significantly greater ( $P \leq 0.01$ ) than that for each single treatment (Fig. 1A, upper panels); as well as consistently and significantly (all  $P \leq 0.05$ ) more than for each of the three dual treatments (Supplemental Fig. 1A). Moreover, comparison of the sum of the effects of each stimulus with the effect of the combined stimulation revealed obvious ( $P \leq 0.05$  and 0.01, respectively) *supra*-additivity between IL-1 $\beta$ , IFN- $\gamma$ , and dexamethasone at both 6 and 24 hours (Fig. 1A, lower panels).

In pHBECs grown in submersion culture, IL-1 $\beta$ , IFN- $\gamma$ , and dexamethasone alone produced low levels of TLR2 protein, whereas treatment with IL-1 $\beta$ +Dex, IL-1 $\beta$ +IFN- $\gamma$ , or IFN- $\gamma$ +Dex each more clearly induced TLR2 protein at 24 hours (Fig. 1B, upper graph). Summation of the effects for each of

these pairs of stimuli (sum) was less ( $P \leq 0.05$ ) than the respective combination effect (comb), and therefore *supra*-additivity is revealed (Fig. 1B, lower graph). In the case of treatment with IL-1 $\beta$ +IFN- $\gamma$ +Dex, TLR2 protein was increased by  $\sim 2100$ -fold ( $P \leq 0.05$ ), and this was to a higher level than for each of IL-1 $\beta$ , IFN- $\gamma$ , or dexamethasone alone (Fig. 1B, upper graph). Comparing the additive effects for each of IL-1 $\beta$ , IFN- $\gamma$ , and dexamethasone (sum) with the combination effect of IL-1 $\beta$ +IFN- $\gamma$ +Dex (comb) showed marked ( $P \leq 0.05$ ) *supra*-additivity between these stimuli on TLR2 protein (Fig. 1B, lower graph).

In pHBECs grown at ALI, whereas each of IL-1 $\beta$ , IFN- $\gamma$ , and budesonide produced little increase in TLR2 protein at both 6 and 24 hours, induction (all  $P \leq 0.01$ ) was produced by IL-1 $\beta$  plus budesonide (IL-1 $\beta$ +Bud) and IL-1 $\beta$  plus IFN- $\gamma$  plus budesonide (IL-1 $\beta$ +IFN- $\gamma$ +Bud) (Supplemental Fig. 2A, upper panels). However, in ALI cultures of pHBECs, none of the combinations of IL-1 $\beta$ , IFN- $\gamma$ , and budesonide revealed statistically significant *supra*-additivity on TLR2 protein at either 6 or 24 hours (Supplemental Fig. 2A, lower panels). Nevertheless, in the case of IL-1 $\beta$ +Bud and IL-1 $\beta$ +IFN- $\gamma$ +Bud, trends toward a greater effect for the combination treatment (comb) compared with the sum of the effects of each stimulus (sum) were apparent.

**Effect of IL-1 $\beta$ , IFN- $\gamma$ , and Glucocorticoid on TLR2 mRNA Expression in Pulmonary Epithelial Cells.** TLR2 mRNA was only marginally induced by IL-1 $\beta$ , IFN- $\gamma$ , or dexamethasone alone at both 6 and 24 hours in A549 cells (Fig. 2A, upper panels). However, the combination of IL-1 $\beta$ +Dex increased TLR2 mRNA at 6 hours in a manner that was greater ( $P \leq 0.01$ ) than simple additivity (Fig. 2A). Similarly, dexamethasone also enhanced IFN- $\gamma$ -induced TLR2 mRNA at 6 and 24 hours such that the effect of cotreatment with IFN- $\gamma$ +Dex (comb) was higher ( $P \leq 0.05$ ) than the sum of the effects of IFN- $\gamma$  and dexamethasone alone (sum) (Fig. 2A). These data indicate *supra*-additivity between IFN- $\gamma$  and dexamethasone on TLR2 mRNA at both 6 and 24 hours. Cotreating A549 cells with IL-1 $\beta$ +IFN- $\gamma$  also led to slight increases in TLR2 mRNA at 6 and 24 hours, although no combinatorial effect of IL-1 $\beta$  and IFN- $\gamma$  on TLR2 mRNA was observed. However, combined stimulation of A549 cells with IL-1 $\beta$ +IFN- $\gamma$ +Dex profoundly induced TLR2 mRNA to 19- and 69-fold at 6 and 24 hours, respectively ( $P \leq 0.001$  and 0.01, respectively) (Fig. 2A, upper panels). Such induction of TLR2 expression was greater (all  $P \leq 0.001$ ) than was evident for IL-1 $\beta$ , IFN- $\gamma$ , or dexamethasone alone at both 6 and 24 hours. Moreover, comparison of the sum of the effects of single treatments with that of the effect of the combined stimulus showed marked ( $P \leq 0.05$  and 0.01, respectively) *supra*-additivity between the effects of IL-1 $\beta$ , IFN- $\gamma$ , and dexamethasone at 6 and 24 hours (Fig. 2A, lower panels). Furthermore, the addition of IL-1 $\beta$ , dexamethasone, or IFN- $\gamma$  to each of the three dual treatments led to reproducible and statistically significant increases in TLR2 mRNA expression at both 6 and 24 hours (Fig. 2A; Supplemental Fig. 1B). Thus, clear positive combinatorial effects between IL-1 $\beta$ , IFN- $\gamma$ , and dexamethasone on TLR2 mRNA expression were revealed in A549 cells.

Similarly, the effects of IL-1 $\beta$ , IFN- $\gamma$ , and glucocorticoid on TLR2 mRNA were investigated in pHBECs. In submersion cultures of pHBECs, TLR2 mRNA was modestly induced by IL-1 $\beta$ , IFN- $\gamma$ , and dexamethasone alone at both 6 and 24 hours (Fig. 2B, upper panels). Treatment with IL-1 $\beta$ +Dex

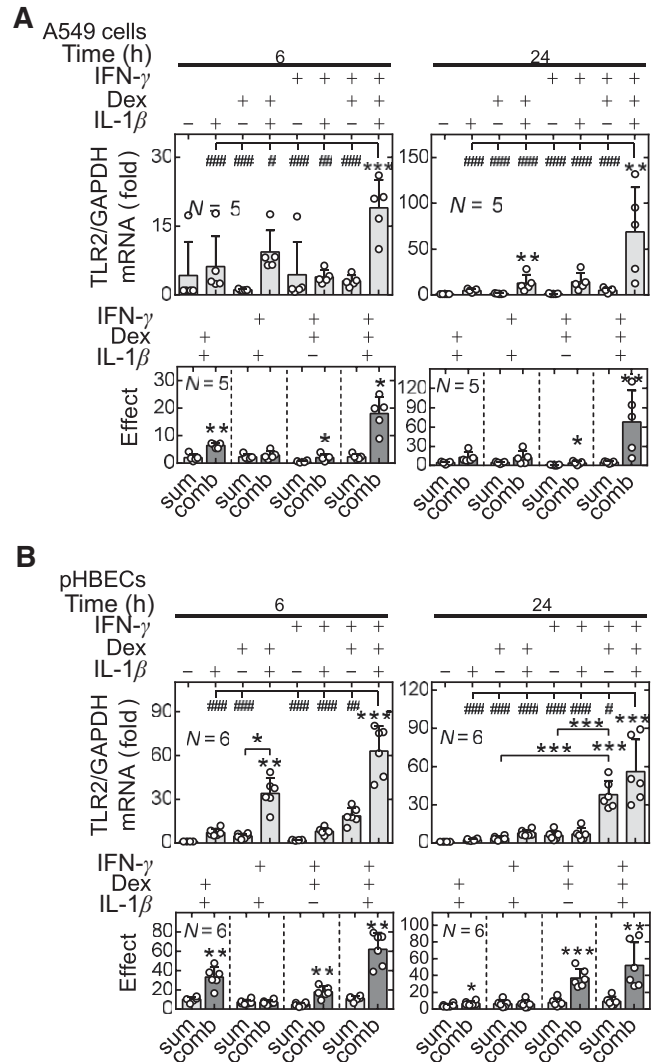


**Fig. 2.** Effect of IL-1 $\beta$ , IFN- $\gamma$  and dexamethasone on TLR2 mRNA in human pulmonary epithelial cells. (A) A549 cells or (B) pHBECs grown in submersion culture were either not treated or treated with IL-1 $\beta$  (1 ng/ml), IFN- $\gamma$  (10 ng/ml), and/or Dex (1  $\mu$ M) as indicated. Cells were harvested at 6 or 24 hours for quantitative polymerase chain reaction analysis of TLR2 and GAPDH. (Upper graphs) TLR2 data from  $N$  independent experiments were normalized to GAPDH, expressed as fold of untreated, and mean  $\pm$  S.D. were plotted as bar graphs with overlaid scatter plots. Significance was tested using ANOVA with a Tukey post hoc test. Asterisks (\*, \*\*, or \*\*\*) represent significance relative to untreated or as indicated. Hash (#, ##, or ###) represent significance relative to IL-1 $\beta$ +IFN- $\gamma$ +Dex. (Lower graphs) The sum of each effect (i.e., fold - 1) within a group of treatments (sum) and the effect (fold - 1) for each combination treatment (comb) is expressed as mean  $\pm$  S.D. and plotted as bar graphs overlaid with scatter plots. Significance was tested using paired  $t$  test. \*, # $P \leq 0.05$ ; \*\*, ## $P \leq 0.01$ ; \*\*\*, ### $P \leq 0.001$ .

induced ( $P \leq 0.01$ ) TLR2 mRNA at 6 hours, and IFN- $\gamma$ +Dex induced ( $P \leq 0.001$ ) TLR2 mRNA at 24 hours (Fig. 2B, upper panels). Although combined stimulation with IL-1 $\beta$ +IFN- $\gamma$  showed little increase in TLR2 mRNA at 6 and 24 hours, dexamethasone enhanced ( $P \leq 0.001$ ) the IL-1 $\beta$ +IFN- $\gamma$ -induced TLR2 mRNA at both times (Fig. 2B, upper panels). Moreover, IL-1 $\beta$ +IFN- $\gamma$ +Dex-induced TLR2 mRNA to 63- and 56-fold at 6 and 24 hours, respectively, and this was more (both  $P \leq 0.01$ ) than each of IL-1 $\beta$ , IFN- $\gamma$ , or dexamethasone alone. Comparison of the effects of the combination treatments (comb), IL-1 $\beta$ +Dex, IFN- $\gamma$ +Dex, or IL-1 $\beta$ +IFN- $\gamma$ +Dex, to the

sum of the effects of the respective individual treatments (sum) revealed obvious (all  $P \leq 0.05$ ) *supra*-additivity at both 6 and 24 hours (Fig. 2B, lower panels).

In ALI cultures of pHBEs, TLR2 mRNA was modestly induced by IL-1 $\beta$  and budesonide alone, and clear combinatorial effects, with *supra*-additivity ( $P \leq 0.05$ ), between IL-1 $\beta$  and budesonide were observed at both 6 and 24 hours (Supplemental Fig. 2B). Although IFN- $\gamma$  barely induced TLR2 expression in the ALIs, cotreatment with IL-1 $\beta$  led to increased ( $P \leq 0.05$ ) TLR2 mRNA at both 6 and 24 hours (Supplemental Fig. 2B, upper panels). Similarly, IFN- $\gamma$ +Bud cotreatment increased ( $P \leq 0.001$ ) TLR2 mRNA above baseline. Moreover, budesonide enhanced ( $P \leq 0.01$ ) IL-1 $\beta$ +IFN- $\gamma$ -induced TLR2 mRNA to 11.6- and 7.8-fold at 6 and 24 hours, respectively. Thus, at both times, TLR2 mRNA induced by the combined stimulation with IL-1 $\beta$ +IFN- $\gamma$ +Bud was higher (all  $P \leq 0.01$ ) than by IL-1 $\beta$ , IFN- $\gamma$ , or budesonide alone (Supplemental Fig. 2B, upper panels). Indeed, comparison of the sum of the effects of IL-1 $\beta$ , IFN- $\gamma$ , and budesonide alone (sum) with the effect of their combined stimulation (comb) revealed *supra*-additivity between IL-1 $\beta$ +IFN- $\gamma$ +Bud at 24 hours ( $P \leq 0.05$ ) but not at 6 hours (Supplemental Fig. 2B, lower panels). However, this synergistic effect was no more than for IL-1 $\beta$ +Bud combination, i.e., IFN- $\gamma$  had no additional effect over IL-1 $\beta$ +Bud combination.

As GAPDH expression may vary with some treatments, cycle threshold ( $C_T$ ) values to show GAPDH expression for all treatments are shown (Supplemental Fig. 3, A–C). In each case, this was unaffected by IL-1 $\beta$ , IFN- $\gamma$ , or dexamethasone treatments in A549, pHBEs, and ALI cultures.

**IKK Involvement in IL-1 $\beta$ +IFN- $\gamma$ +Dex-Induced TLR2 Expression.** Prior work showed a role for NF- $\kappa$ B in the induction of TLR2 by IL-1 $\beta$  plus glucocorticoid (Bansal et al., 2022). Here, a role for the canonical IKK pathway, involving IKK2, in the IL-1 $\beta$ +IFN- $\gamma$ +Dex-induced TLR2 expression was tested in A549 cells using the IKK2-selective inhibitors PS-1145, ML120B, and TPCA-1 (Gamble et al., 2012). For each compound, concentrations of 30  $\mu$ M produced maximal inhibition of IL-1 $\beta$ -induced NF- $\kappa$ B luciferase reporter activity (Fig. 3A; Supplemental Fig. 4A).

TLR2 mRNA and protein expression were modestly induced by IFN- $\gamma$ +Dex, at 6 and 24 hours, and these effects were significantly enhanced ( $P \leq 0.001$  and 0.01, respectively) by IL-1 $\beta$  (Fig. 3, B and C). In cells pretreated with 30  $\mu$ M PS-1145, ML120B, or TPCA-1, the enhancement of IFN- $\gamma$ +Dex-induced TLR2 mRNA and protein by IL-1 $\beta$  were reduced (all  $P \leq 0.05$ ) by each compound (Fig. 3, B and C). In each case, PS-1145 and ML120B produced partial inhibition, whereas TPCA-1 resulted in more complete inhibition of TLR2 mRNA and protein expression. Neither of these compounds affected the cell viability in the experimental conditions employed (Supplemental Fig. 4B). These data support a role, albeit possibly only partial, for IKK2 in the induction of TLR2 expression by IL-1 $\beta$ +IFN- $\gamma$ +Dex.

Effects of IFN- $\gamma$  on the possible activation of NF- $\kappa$ B were also examined. Treatment of A549 cells with IFN- $\gamma$  did not elicit serine 32 and 36 phosphorylation of I $\kappa$ B $\alpha$  (Supplemental Fig. 4C). Likewise, IFN- $\gamma$  alone did not induce NF- $\kappa$ B reporter activity and showed no effect on IL-1 $\beta$ -induced NF- $\kappa$ B reporter activity whether in the absence or presence of dexamethasone (Supplemental Fig. 4D, top panel). Thus, although IKK2 is implicated in the induction of TLR2 expression by

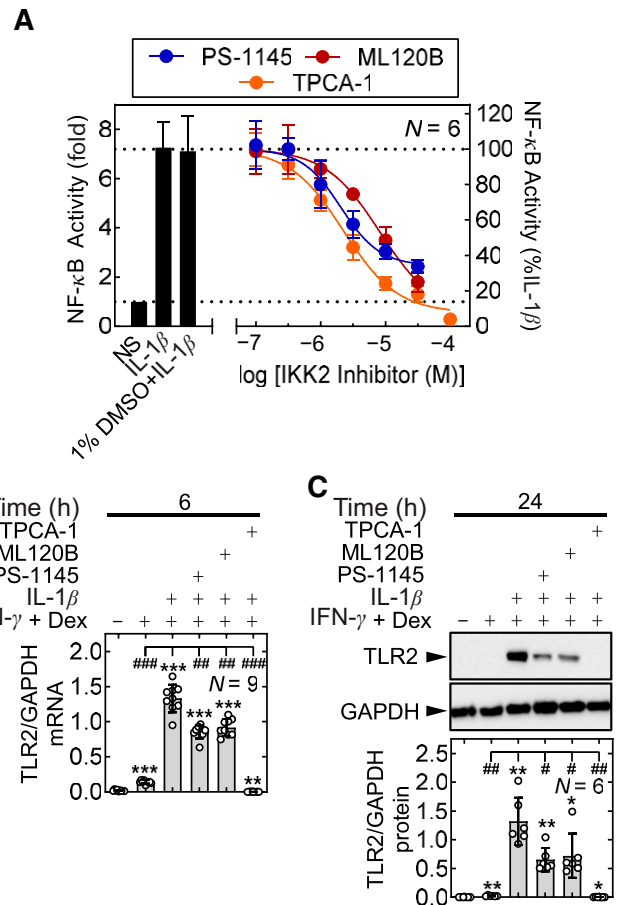


**Fig. 3.** Effect of IKK inhibitors on the enhancement of IFN- $\gamma$ +Dex-induced TLR2 expression by IL-1 $\beta$ . (A) A549 cells containing the NF- $\kappa$ B reporter 6 $\kappa$ Btk.luc were either not treated or pretreated with 1% DMSO or indicated concentrations of PS-1145, ML120B, or TPCA-1 for 90 minutes prior to stimulation with IL-1 $\beta$  (1 ng/ml). Cells were harvested for luciferase assay. Data from  $N$  independent experiments was expressed as fold (bars) and percent IL-1 $\beta$  (lines) and plotted as mean  $\pm$  S.D. Scatterplots showing individual data points appear as Supplemental Fig. 4A. (B) A549 cells were pretreated with PS-1145, ML120B, or TPCA-1, each at 30  $\mu$ M, for 1.5 hours prior to stimulation with IFN- $\gamma$  (10 ng/ml) plus Dex (1  $\mu$ M) and IL-1 $\beta$  (1 ng/ml) as indicated. Cells were harvested at 6 hours for RNA extraction and quantitative polymerase chain reaction analysis of TLR2 and GAPDH mRNA. (C) Cells were treated as in (B) and harvested at 24 hours for western blot analysis of TLR2 and GAPDH protein. (B and C) TLR2 data, from  $N$  independent experiments, were normalized to GAPDH and are expressed as mean  $\pm$  S.D. and plotted as bar graphs overlaid with scatter plots. Significance was assessed by ANOVA with a Tukey multiple comparison test. Differences from untreated: \* $P \leq 0.05$ ; \*\* $P \leq 0.01$ ; \*\*\* $P \leq 0.001$ ; from IL-1 $\beta$ +IFN- $\gamma$ +Dex: # $P \leq 0.05$ ; ## $P \leq 0.01$ ; ### $P \leq 0.001$ .

IL-1 $\beta$ +IFN- $\gamma$ +Dex, there was no effect of IFN- $\gamma$  on activation of the NF- $\kappa$ B pathway or the induction of NF- $\kappa$ B transcriptional activity.

**Involvement of GR in IL-1 $\beta$ +IFN- $\gamma$ +Dex-Induced TLR2 Expression.** A role for GR in the synergistic induction of TLR2 expression by IL-1 $\beta$  plus glucocorticoid was previously documented (Bansal et al., 2022). In the current study, the role of GR in the induction of TLR2 expression by IL-1 $\beta$ +IFN- $\gamma$ +Dex was tested using the competitive GR antagonist Org34517 (Peeters et al., 2004; Joshi et al., 2015a). TLR2 mRNA and protein were both modestly induced by IL-1 $\beta$ +IFN- $\gamma$  at 6 and 24 hours, respectively (Fig. 4, A and B;

Supplemental Fig. 5, A and B). Increasing the concentration of dexamethasone markedly enhanced IL-1 $\beta$ +IFN- $\gamma$ -induced TLR2 mRNA at 6 hours and protein at 24 hours. In each case, these enhancements by dexamethasone were competitive with Org34517, at 1  $\mu$ M, as shown by rightward shifts in the response curve to dexamethasone (Fig. 4, A and B). Schild analysis to determine the negative logarithm of the molar concentration of antagonist that causes a twofold shift of the concentration-response curve for agonist, or  $pA_2$  value, resulted in  $pA_2$  values of  $8.07 \pm 0.16$  and  $7.85 \pm 0.29$  for TLR2 mRNA and protein, respectively, which is consistent with prior reports of competitive antagonism at GR. IL-1 $\beta$ +IFN- $\gamma$ -induced TLR2 mRNA and protein were unaffected by Org34517.

Possible effects of IL-1 $\beta$  and IFN- $\gamma$  on GRE-dependent transcriptional activity were investigated using A549 cells harboring a 2 $\times$ GRE.luc reporter. GRE reporter activity was not induced by either IL-1 $\beta$  or IFN- $\gamma$  and following induction by dexamethasone at 6 hours; reporter activity also remained largely unaffected by IL-1 $\beta$  and IFN- $\gamma$  treatments (Supplemental Fig. 4D, middle panel). Thus, although the antagonism by Org34517 supports a role for GR in the induction of TLR2 by IL-1 $\beta$ +IFN- $\gamma$ +Dex, GRE reporter activity was unaffected by IL-1 $\beta$  and/or IFN- $\gamma$ , suggesting that an enhancement of simple GRE-dependent transcription does not directly contribute to the observed synergy in respect of TLR2 expression.

**Activation of JAK-STAT Signaling by IFN- $\gamma$ .** STAT1 is the major transcription factor involved in IFN- $\gamma$ -dependent transcriptional responses that occur via conventional JAK-STAT signaling (Schroder et al., 2004). To explore possible activation of STAT1, IFN- $\gamma$ -induced phosphorylation of STAT1 at Y701 and S727, which are suggested to be involved in nuclear accumulation and transcriptional activation, respectively, were examined (Sadzak et al., 2008). Treatment of A549 cells with IFN- $\gamma$  at 10 ng/ml induced rapid phosphorylation of STAT1 at Y701, with statistical significance observed from 15 minutes onwards (Fig. 5A; Supplemental Fig. 6A). This peaked at 1 hour before declining slightly by 6 and 24 hours. Phosphorylation of STAT1 at S727 was detectable in unstimulated cells, and this was increased ( $P \leq 0.05$ ) by 1 hour post IFN- $\gamma$  treatment (Fig. 5B; Supplemental Fig. 6B). This phosphorylation declined slightly by 6 hours but was further elevated at 24 hours. However, although total STAT1 levels were unaffected by IFN- $\gamma$  treatment at times until 6 hours, there was a  $\sim$ twofold ( $P \leq 0.05$ ) increase in total STAT1 at 24 hours (Fig. 5B; Supplemental Fig. 6B). This effect largely accounts for the increase in S727 phosphorylation observed at 24 hours. Overall, these data indicate activation of STAT1 by IFN- $\gamma$ .

The effects of IL-1 $\beta$ , IFN- $\gamma$ , and dexamethasone were tested on phosphorylation of STAT1 at Y701 and S727 at 1 hour. STAT1 phosphorylation at Y701 was not induced by IL-1 $\beta$ , either in the presence or absence of dexamethasone (Fig. 5C, upper panels). IFN- $\gamma$  strongly ( $P \leq 0.05$ ) induced STAT1 phosphorylation at Y701, and this was unaffected by the addition of IL-1 $\beta$  and/or dexamethasone (Fig. 5C, upper panels). Although dexamethasone did not induce STAT1 S727 phosphorylation, IL-1 $\beta$  alone induced ( $P \leq 0.01$ ) levels of S727 phosphorylated STAT1 that remained high with IL-1 $\beta$ +Dex cotreatment (Fig. 5C, lower panels). IFN- $\gamma$  alone also induced ( $P \leq 0.01$ ) STAT1 S727 phosphorylation, and this was unchanged with IFN- $\gamma$ +Dex cotreatment (Fig. 5C,

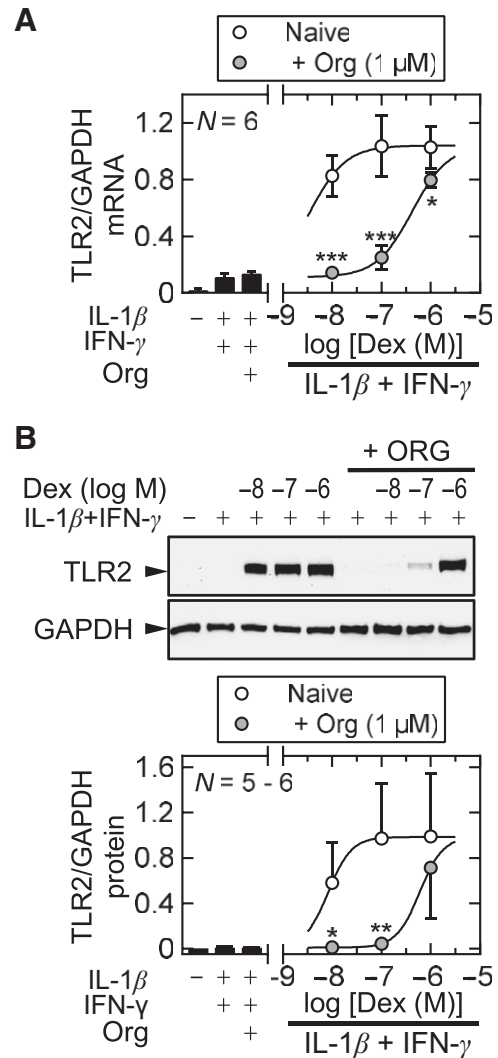


**Fig. 4.** Effect of Org34517 (Org) on the enhancement of IL-1 $\beta$ +IFN- $\gamma$ -induced TLR2 expression by dexamethasone. A549 cells were pre-treated with Org34517 (1  $\mu$ M) for 1 hour prior to stimulation with IL-1 $\beta$  (1 ng/ml) plus IFN- $\gamma$  (10 ng/ml) in the absence or presence of various concentrations of Dex. (A) After 6 hours, cells were harvested for RNA extraction and quantitative polymerase chain reaction analysis of TLR2 and GAPDH mRNA. (B) At 24 hours, cells were harvested for western blot analysis of TLR2 and GAPDH. In each case, TLR2 data, from  $N$  independent experiments, were normalized to GAPDH and are plotted as means  $\pm$  S.D. Significance between treatments without and with Org was assessed by paired  $t$  test (two tailed). Note: unpaired  $t$  test was used at 0.1  $\mu$ M Dex due to one sample failure in the western blotting. \* $P \leq 0.05$ ; \*\* $P \leq 0.01$ ; \*\*\* $P \leq 0.001$ . For illustration, curves were fitted following Schild analysis that assumed a common maximal effect ( $E_{max}$ ) and a Schild slope factor of 1, with the lower asymptote fixed as the response to IL-1 $\beta$ +IFN- $\gamma$ . This produced  $pA_2$  values of  $8.07 (\pm 0.16)$  and  $7.85 (\pm 0.29)$  for TLR2 mRNA and protein, respectively. Scatterplots for all data in (A) and (B) are shown as Supplemental Fig. 5, A and B.

lower panels). Combination of IL-1 $\beta$ +IFN- $\gamma$  increased S727 STAT1 phosphorylation to a higher level than either IL-1 $\beta$  or IFN- $\gamma$  alone, both  $P \leq 0.01$ , and this was unaffected by dexamethasone (Fig. 5C, lower panels). Total STAT1 expression was not affected by IL-1 $\beta$ , IFN- $\gamma$ , or dexamethasone whether alone or in combination (Supplemental Fig. 7A). Overall, these data show increased STAT1 phosphorylation at Y701 and S727 following IFN- $\gamma$  treatment. S727 phosphorylation was also increased by IL-1 $\beta$ , and this appeared to be additive

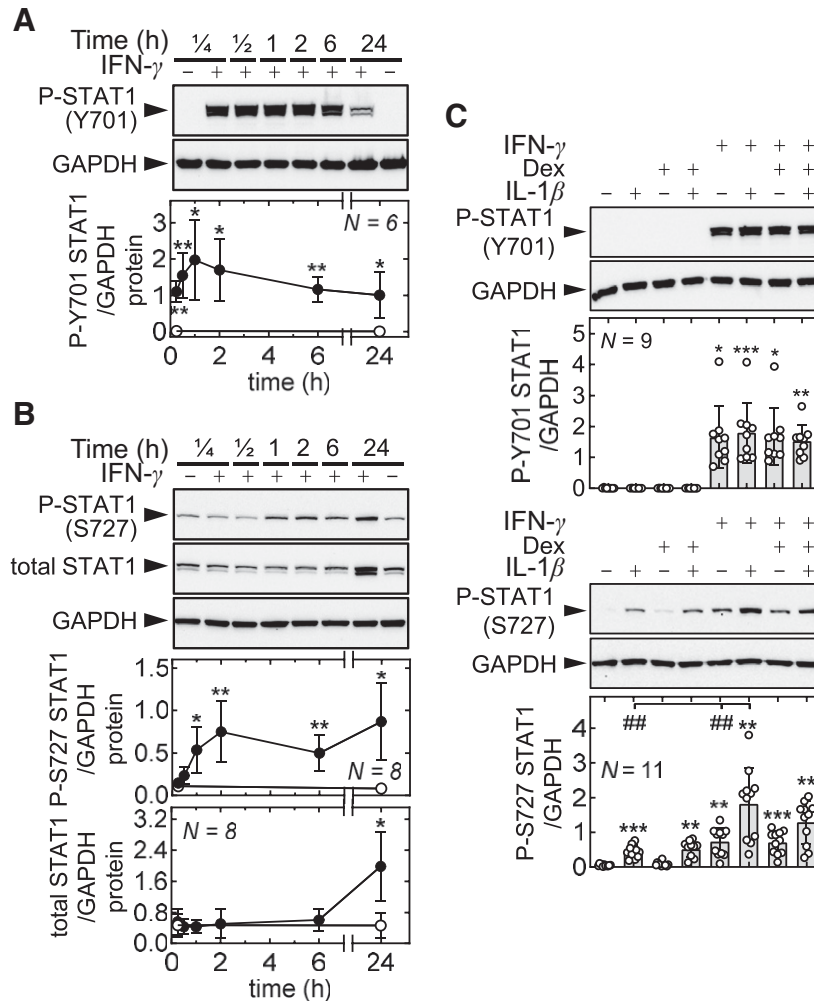


**Fig. 5.** Effect of IL-1 $\beta$ , glucocorticoid, and IFN- $\gamma$  on STAT1 phosphorylation. A549 cells were either untreated or treated with IFN- $\gamma$  (10 ng/ml) prior to harvesting for western blot analysis at the indicated times. Representative blots of (A) phospho-STAT1 (P-STAT1 Y701) and GAPDH and (B) P-STAT1 (S727), total STAT1, and GAPDH from *N* independent experiments are shown. In each case, densitometric data normalized to GAPDH are plotted as means  $\pm$  S.D. (error bars). Significance relative to untreated at 15 minutes was assessed by ANOVA with a Dunnett's multiple comparison test. (C) A549 cells were either not treated or treated with IL-1 $\beta$  (1 ng/ml), IFN- $\gamma$  (10 ng/ml), and/or Dex (1  $\mu$ M) as indicated. Cells were harvested at 1 hour for western blot analysis of P-STAT1 (Y701 and S727) and GAPDH. Representative blots of P-STAT1 (Y701 & S727) and GAPDH from *N* independent experiments are shown. Densitometric data for P-STAT1 (Y701) (upper graph) and P-STAT1 (S727) (lower graph) were normalized to GAPDH, expressed as means  $\pm$  S.D., and plotted as bar graphs overlaid with scatter plots. Significance relative to untreated (\*) or IL-1 $\beta$ +IFN- $\gamma$  (#) was tested using ANOVA with a Tukey post hoc test. \*,  $P \leq 0.05$ ; \*\*,  $##P \leq 0.01$ ; \*\*\*,  $###P \leq 0.001$ . Scatterplots for all data in (A) and (B) are shown as Supplemental Fig. 6.

with the effect of IFN- $\gamma$ . In each case, dexamethasone, alone or in combination with IL-1 $\beta$  and/or IFN- $\gamma$ , did not affect STAT1 phosphorylation at Y701 and S727.

To test for possible JAK involvement, the JAK inhibitors AZD1480, baricitinib, and ruxolitinib were tested on the ability of IFN- $\gamma$  to induce STAT1 phosphorylation. IFN- $\gamma$ -induced phosphorylation of STAT1 at Y701 and S727 was prevented by each JAK inhibitor in a concentration-dependent manner (Fig. 6, A–C; Table 1). Inserts in Fig. 6C provide the log EC<sub>50</sub> values obtained for each pair of curves describing the effect of each compound on S727 and Y701 phosphorylated STAT1 in each individual experiment (Fig. 6C). Both AZD1480 and baricitinib revealed greater ( $P \leq 0.01$  and  $0.05$ , respectively) sensitivity of inhibition in respect of S727 compared with Y701 phosphorylation of STAT1. With ruxolitinib, this effect was much reduced, and although reaching  $P = 0.049$ , it should be noted that one set of data were excluded (Supplemental Fig. 8). The apparent difference in log EC<sub>50</sub> values should therefore

be treated with caution. Total STAT1 expression remained unaffected by the various concentrations of JAK inhibitors in the presence of IFN- $\gamma$  (data not shown). Furthermore, unstimulated A549 cells showed lower levels of STAT1 phosphorylation at S727, and these were unaffected by 1  $\mu$ M of each of the JAK inhibitors (Fig. 6D, left panel). IL-1 $\beta$  treatment increased STAT1 S727 phosphorylation compared with baseline, which also remained unaffected by the JAK inhibitors (Fig. 6D, left panel). Treatment with IFN- $\gamma$  increased STAT1 phosphorylation at S727, and this was completely abrogated to baseline by the JAK inhibitors (Fig. 6D, right panel). Treatment with IL-1 $\beta$ +IFN- $\gamma$  induced S727 phosphorylation to a greater level than IFN- $\gamma$  alone, and each JAK inhibitor partially, but significantly (all  $P \leq 0.05$ ), reduced this response (Fig. 6D, right panel). As stated above, STAT1 phosphorylation at Y701 was not observed in unstimulated or IL-1 $\beta$ -treated A549 cells, and this was not changed by the JAK inhibitors (data not shown). IFN- $\gamma$  and IL-1 $\beta$ +IFN- $\gamma$  treatments strongly induced similar



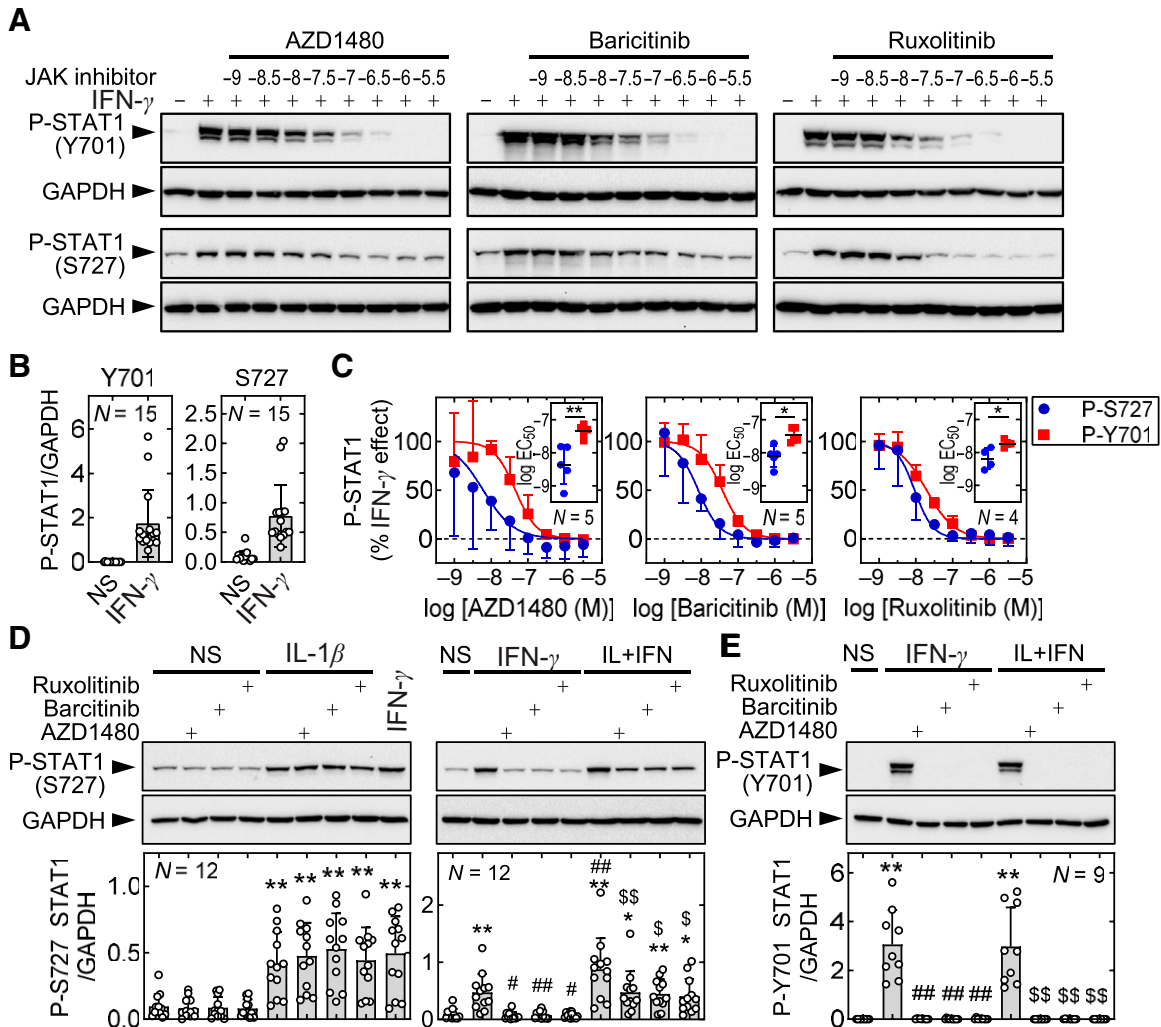


**Fig. 6.** Effect of JAK inhibitors on STAT1 phosphorylation. (A) A549 cells were pretreated with AZD1480, baricitinib and ruxolitinib at the indicated concentrations for 30 minutes, followed by stimulation with IFN- $\gamma$  (10 ng/ml) for 1 hour. Cells were harvested for western blot analysis of phospho-STAT1 (P-STAT1) and GAPDH. Representative blots for P-STAT1 (Y701), P-STAT1 (S727), and GAPDH from five independent experiments are shown. (B) Densitometric data for Y701 P-STAT1 and S727 P-STAT1 from western blots shown in (A) were normalized to GAPDH and plotted as mean  $\pm$  S.D. (C) Data were expressed as percent IFN- $\gamma$  effect for each of AZD1480, baricitinib, and ruxolitinib and plotted as means  $\pm$  S.D. and shown as scatter plots in the inserts within each graph of (C). Note: one dataset was excluded for ruxolitinib, and the full data are shown as Supplemental Fig. 8. (D and E) A549 cells were either not treated or pretreated with AZD1480, baricitinib, and ruxolitinib, each at 1  $\mu$ M, for 1 hour prior to stimulation with IL-1 $\beta$  (1 ng/ml) and IFN- $\gamma$  (10 ng/ml) as indicated. Cells were harvested at 1 hour for western blot analysis of P-STAT1 and GAPDH. Representative blots for P-STAT1 (Y701 & S727) and GAPDH from *N* independent experiments are shown. Densitometric data for (D) P-STAT (S727) and (E) P-STAT1 (Y701) were normalized to GAPDH, expressed as means  $\pm$  S.D., and plotted as bar graphs overlaid with scatter plots. Significance relative to untreated (\*), IFN- $\gamma$  (#), or IL-1 $\beta$  + IFN- $\gamma$  (\$) was tested using ANOVA with a Tukey post hoc test. \*, #, \$,  $P \leq 0.05$ ; \*\*, ##, \$\$,  $P \leq 0.01$ ; \*\*\*, ###, \$\$\$,  $P \leq 0.001$ .

levels of STAT1 Y701 phosphorylation, and this induction was completely prevented by all three JAK inhibitors (Fig. 6E). Total STAT1 expression was unaffected by IL-1 $\beta$ , IFN- $\gamma$ , or IL-1 $\beta$ +IFN- $\gamma$  treatments either in the presence or absence of JAK inhibitors (Supplemental Fig. 7B). Although these data support the involvement of JAKs in the activation of STAT1 by IFN- $\gamma$ , whether in the presence or absence of IL-1 $\beta$ , the apparent differences in selectivity on phosphorylation of STAT1 at Y701 versus S727 raise the possibility of mechanistic differences in each process.

#### Activation of STAT1-Driven Transcription by IFN- $\gamma$ .

To explore the transcriptional activation of STAT1 by IFN- $\gamma$ , A549 cells harboring a luciferase reporter containing three consensus STAT1 motifs, corresponding to a conventional GAS, upstream of a luciferase gene driven by a basal promoter

(3 $\times$ STAT1.luc), were stimulated with various concentrations of IFN- $\gamma$  (Fig. 7A; Supplemental Fig. 9A). Reporter activity, measured at 6 hours, was induced by IFN- $\gamma$  in a concentration-dependent manner ( $EC_{50}$  = 0.28 ng/ml), with maximal activity

TABLE 1

Concentration-response analysis of JAK inhibitors on IFN- $\gamma$ -induced STAT1 phosphorylation and STAT1 reporter activity.  $pEC_{50}$  values of the three JAK inhibitors, AZD1480, baricitinib, and ruxolitinib, on inhibition of P-Y701 STAT1, P-S727 STAT1, and STAT1 reporter activity in IFN- $\gamma$ -treated A549 cells are shown (related to Figs. 6, A–C and 7E). Data from four to five independent experiments are shown.

	AZD1480	Baricitinib	Ruxolitinib
Y701	7.3 $\pm$ 0.2	7.4 $\pm$ 0.1	8.0 $\pm$ 0.1
S727	8.2 $\pm$ 0.1	8.1 $\pm$ 0.1	8.2 $\pm$ 0.1
3 $\times$ STAT1.luc	7.1 $\pm$ 0.1	6.9 $\pm$ 0.2	7.0 $\pm$ 0.2

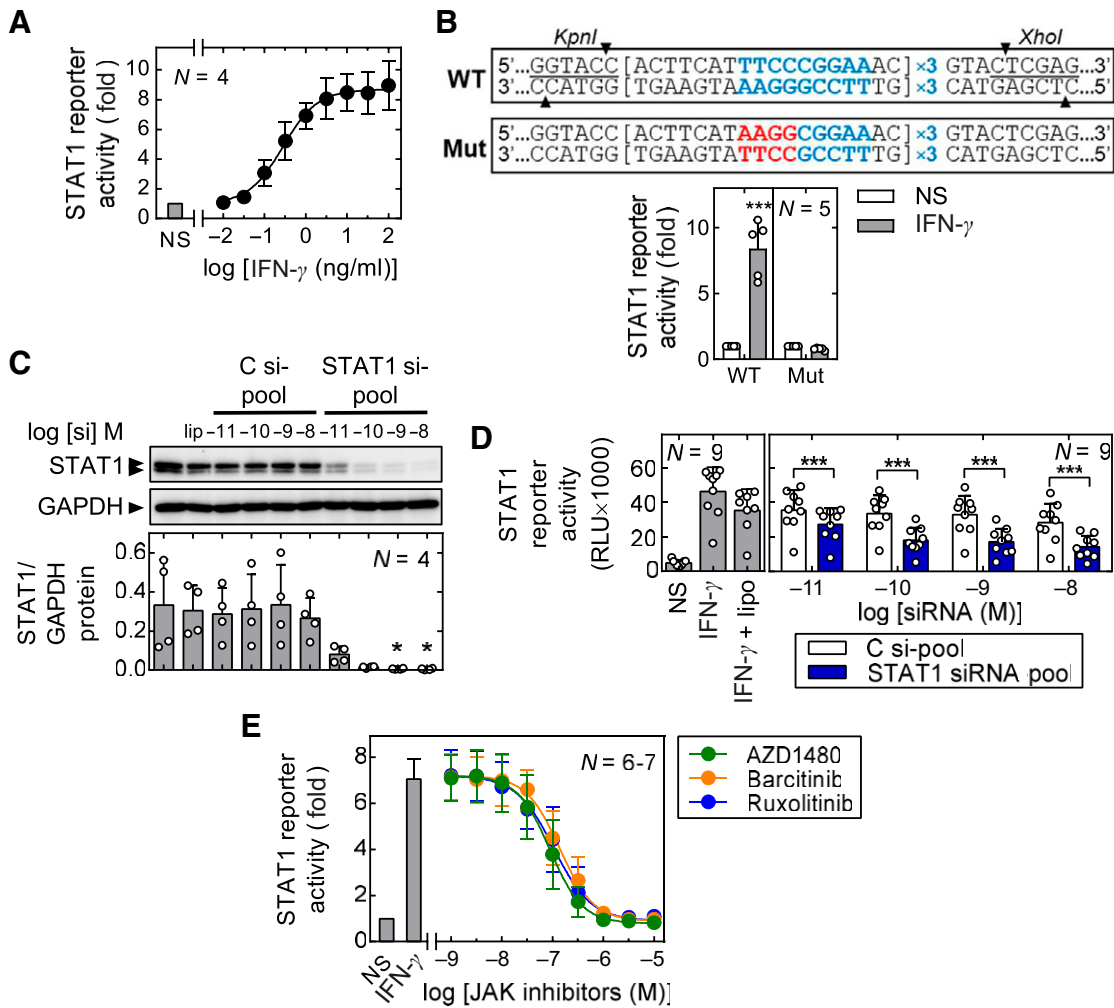


**Fig. 7.** Characterization of a STAT1-driven luciferase reporter. (A) A549 cells stably transfected with a luciferase reporter containing three copies of a consensus STAT1-binding motif [shown in (B)] were either not stimulated (NS) or stimulated with the indicated concentrations of IFN- $\gamma$  prior to harvesting for luciferase assay after 6 hours. Luciferase activity from  $N$  independent experiments was expressed as fold of NS and plotted as mean  $\pm$  S.D. (B) (Upper panel) reporter construct showing three copies of the consensus/wild-type (WT; bold blue) or mutant (Mut; bold blue + red) STAT1-binding motif is shown. *KpnI* and *XhoI* restriction sites used to clone the construct in pGL3.TATA.neo vector are underlined, with cut sites shown as black arrowheads. (Lower panel) A549 cells were stably transfected with the WT or Mut STAT1 reporter constructs and either NS or treated with IFN- $\gamma$  (10 ng/ml) for 6 hours followed by harvesting for luciferase assay. Luciferase activity from  $N$  independent experiments was expressed as fold of NS, and mean  $\pm$  S.D. was plotted as bar graphs overlaid with scatter plots. Significance relative to untreated cells was determined using paired  $t$  test. (C) A549 cells were either NS or incubated with lipid control (lip) alone or with the indicated concentrations of either control siRNA pool (C si-pool), or STAT1 siRNA pool (STAT1 si-pool) for 48 hours. Cells were then incubated overnight with serum-free media prior to harvesting for western blot analysis. Representative blots of STAT1 and GAPDH from  $N$  independent experiments are shown. Data obtained from densitometry analysis were normalized to GAPDH, and mean  $\pm$  S.D. was plotted as bar graphs overlaid with scatter plots. Significance relative to C si-pool at each siRNA concentration was tested by paired  $t$  test. \* $P \leq 0.05$ ; \*\* $P \leq 0.01$ ; \*\*\* $P \leq 0.001$ . (D) A549 cells stably transfected with the WT STAT1 reporter construct were treated with lipid or siRNAs as described in (C) prior to stimulation with IFN- $\gamma$  (10 ng/ml) for 6 hours. Cells were harvested for luciferase assay, and raw luciferase units (RLU) from  $N$  independent experiments were expressed as mean  $\pm$  S.D. and plotted as bar graphs overlaid with scatter plots. Significance relative to C si-pool at each siRNA concentration was tested by paired  $t$  test. (E) A549 cells stably transfected with the WT STAT1 reporter construct were either NS or pretreated with the indicated concentrations of AZD1480, baricitinib, or ruxolitinib for 30 minutes followed by stimulation with IFN- $\gamma$  (10 ng/ml). Cells were harvested for luciferase assay after 6 hours. Luciferase activity from  $N$  independent experiments was expressed as fold of NS and plotted as mean  $\pm$  S.D. Scatterplots for all data in (A) and (E) are shown as Supplemental Fig. 9.

occurring at  $\sim 10$  ng/ml. This correlated with the concentration of IFN- $\gamma$  that showed maximal synergy with IL-1 $\beta$  and glucocorticoid on the induction of TLR2 expression. To confirm a role for the consensus STAT1 motifs in the induction of reporter activity, A549 cells were stably transfected with a reporter construct in which the 3 $\times$ STAT1 motifs were replaced with mutated sites (Fig. 7B, top panel). As above, IFN- $\gamma$ , at 10 ng/ml, induced ( $P \leq 0.001$ ) 3 $\times$ STAT1.luc reporter activity, whereas cells containing the mutated STAT1 reporter showed no enhancement of reporter activity (Fig. 7B, bottom panel). These

data indicate that the consensus STAT1 motif conferred IFN- $\gamma$  inducibility. To confirm a role for STAT1 in IFN- $\gamma$ -induced reporter activity, A549 cells were transfected with various concentrations of four different STAT1-targeting siRNAs, or a pool of STAT1 siRNAs, alongside a pool of nontargeting siRNAs as a control. Although the nontargeting control siRNAs had no effect, each individual STAT1-targeting siRNA dramatically reduced STAT1 protein expression, with maximal effects apparent at 1 and 10 nM (Fig. 7C; Supplemental Fig. 10). A pool of these four STAT1-targeting siRNAs also reduced

( $P \leq 0.05$ ) STAT1 protein expression by  $\sim 90\%$  at both 1 and 10 nM (Fig. 7C). Furthermore, IFN- $\gamma$ -induced STAT1 reporter was unaffected by various concentrations of the control siRNA pool, whereas the STAT1 siRNA pool markedly diminished ( $P \leq 0.001$ ) reporter activity at all siRNA concentrations (Fig. 7D). This confirms the involvement of STAT1 in the activation of this reporter by IFN- $\gamma$ . Moreover, in A549.3 $\times$ STAT1.luc cells pretreated with various concentrations of the JAK inhibitors AZD1480, baricitinib, and ruxolitinib, IFN- $\gamma$ -induced STAT1 transcriptional activity was abrogated in a concentration-dependent manner ( $pEC_{50} = 7.05 \pm 0.22$ ,  $6.86 \pm 0.21$ , and  $6.98 \pm 0.19$  for AZD1480, baricitinib, and ruxolitinib, respectively) (Fig. 7E; Supplemental Fig. 9B). These data confirm that IFN- $\gamma$  activates a JAK pathway and leads to STAT1-dependent transcription via consensus STAT1 motifs.

**Involvement of JAK Signaling in IL-1 $\beta$ +IFN- $\gamma$ +Dex-Induced TLR2 Expression.** To investigate a possible role for JAKs in IL-1 $\beta$ +IFN- $\gamma$ +Dex-induced TLR2 expression, A549 cells were pretreated for 1 hour with AZD14580, baricitinib, and ruxolitinib (each at 1  $\mu$ M) prior to stimulation with IL-1 $\beta$ , IFN- $\gamma$ , and dexamethasone. TLR2 mRNA and protein were modestly induced by IL-1 $\beta$ +Dex at 6 and 24 hours, respectively, and this was markedly enhanced (both  $P \leq 0.01$ ) by IFN- $\gamma$  (Fig. 8). AZD14580, baricitinib, and ruxolitinib each reduced the enhancement of IL-1 $\beta$ +Dex-induced TLR2 mRNA by IFN- $\gamma$  back to the level achieved by IL-1 $\beta$ +Dex (Fig. 8A). As similar data were also obtained for TLR2 protein (Fig. 8B), these data support involvement of JAK signaling in the enhancement of IL-1 $\beta$ +Dex-induced TLR2 expression by IFN- $\gamma$ .

The effect of IL-1 $\beta$  and dexamethasone on IFN- $\gamma$ -induced STAT1 transcriptional activity was also investigated using the A549.3 $\times$ STAT1.luc cells. IL-1 $\beta$  and dexamethasone did not induce STAT1 reporter activity. IFN- $\gamma$  treatment induced strong activation of STAT1 reporter that was modestly, but significantly ( $P \leq 0.05$ ), repressed by IL-1 $\beta$  and largely unaffected by dexamethasone (Supplemental Fig. 4D, lower panel). Since IFN- $\gamma$ -induced STAT1 reporter activity was either not affected or reduced by IL-1 $\beta$  and/or dexamethasone, simple effects on STAT1-dependent transcription by combined stimulation of IL-1 $\beta$ +IFN- $\gamma$ +Dex is unlikely to explain the synergy observed between IL-1 $\beta$ , IFN- $\gamma$ , and dexamethasone at inducing TLR2 expression.

**Roles of p65, GR, and STAT1 on TLR2 Expression Induced by IL-1 $\beta$ , IFN- $\gamma$ , and Dexamethasone.** As shown in Supplemental Fig. 4D, IL-1 $\beta$ -induced NF- $\kappa$ B reporter activity was unaltered by IFN- $\gamma$  and/or dexamethasone. Similarly, as seen above, dexamethasone-induced GRE reporter activity was not affected by IL-1 $\beta$  and/or IFN- $\gamma$ . Likewise, IFN- $\gamma$ -induced STAT1 reporter activity was also unaffected by IL-1 $\beta$  and/or dexamethasone. Therefore, the effects of IL-1 $\beta$  on GR and STAT1 signaling, or of dexamethasone on NF- $\kappa$ B and JAK-STAT pathway, or of IFN- $\gamma$  on the NF- $\kappa$ B or GR signaling, do not explain the synergy between IL-1 $\beta$ , IFN- $\gamma$ , and dexamethasone at the level of TLR2 expression. Nevertheless, the involvement of p65, GR, and STAT1 transcription factors, as the primary factors activated by each pathway, seems highly plausible in the synergy in TLR2 expression by combined stimulation with IL-1 $\beta$ , IFN- $\gamma$ , and dexamethasone. This was tested by knocking down the expression of each factor. To confirm the knockdown of p65, A549 cells were transfected with various concentrations of

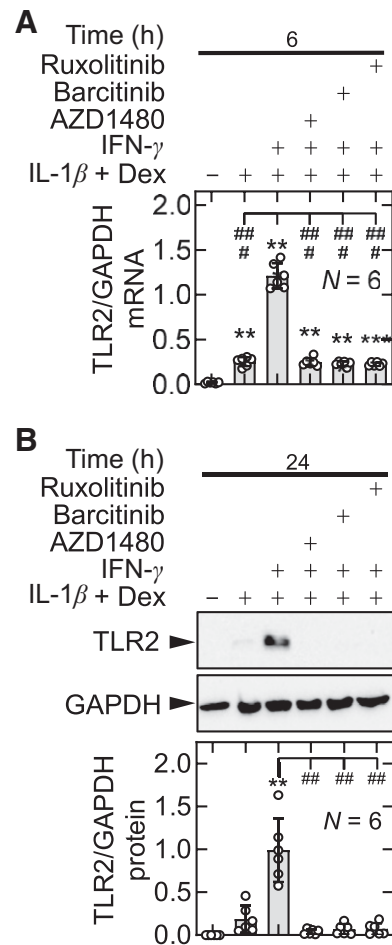


**Fig. 8.** Effect of JAK inhibitors on the enhancement of IL-1 $\beta$ +Dex-induced TLR2 expression by IFN- $\gamma$ . A549 cells were either not stimulated or pretreated with AZD1480, baricitinib, or ruxolitinib, each at 1  $\mu$ M, for 1 hour prior to stimulation with IL-1 $\beta$  (1 ng/ml) plus Dex (1  $\mu$ M) and IFN- $\gamma$  (10 ng/ml) as indicated. (A) Cells were harvested at 6 hours for RNA extraction and quantitative polymerase chain reaction analysis of TLR2 and GAPDH mRNA. (B) Cells were harvested at 24 hours for western blot analysis of TLR2 and GAPDH protein. In each case, TLR2 data, from  $N$  independent experiments, were normalized to GAPDH, and mean  $\pm$  S.D. were plotted as bar graphs overlaid with scatter plots. Significance was assessed by ANOVA with a Tukey multiple comparison test. Differences from untreated: \*\* $P \leq 0.01$ ; \*\*\* $P \leq 0.001$ ; from IL-1 $\beta$ +IFN- $\gamma$ +Dex: ### $P \leq 0.01$ ; #### $P \leq 0.001$ .

four different p65-targeting siRNAs, or a pool of p65 siRNAs, alongside a pool of nontargeting siRNAs as a control. Although the nontargeting control siRNAs had no effect on p65 protein expression, each individual p65-targeting siRNA, as well as the p65 siRNA pool, dramatically reduced p65 protein expression at 1 and 10 nM (Supplemental Fig. 11A). NF- $\kappa$ B reporter activity was also tested to assess the effectiveness of the p65 knockdown. Thus, increasing concentrations of each of the p65 siRNAs, along with the p65 siRNA pool, reduced the IL-1 $\beta$ -induced NF- $\kappa$ B reporter activity, where the greatest effect was observed at 1 and 10 nM, and the nontargeting control siRNAs had no effect (Supplemental Fig. 11B). To achieve knockdown of GR, siRNAs used in a prior study were employed (Thorne et al., 2023). Further, the role of each of p65, GR, and STAT1 was tested on TLR2 expression. Therefore, A549 cells were transfected with siRNA pools targeting each of p65, GR, and/or STAT1, followed by treatment with

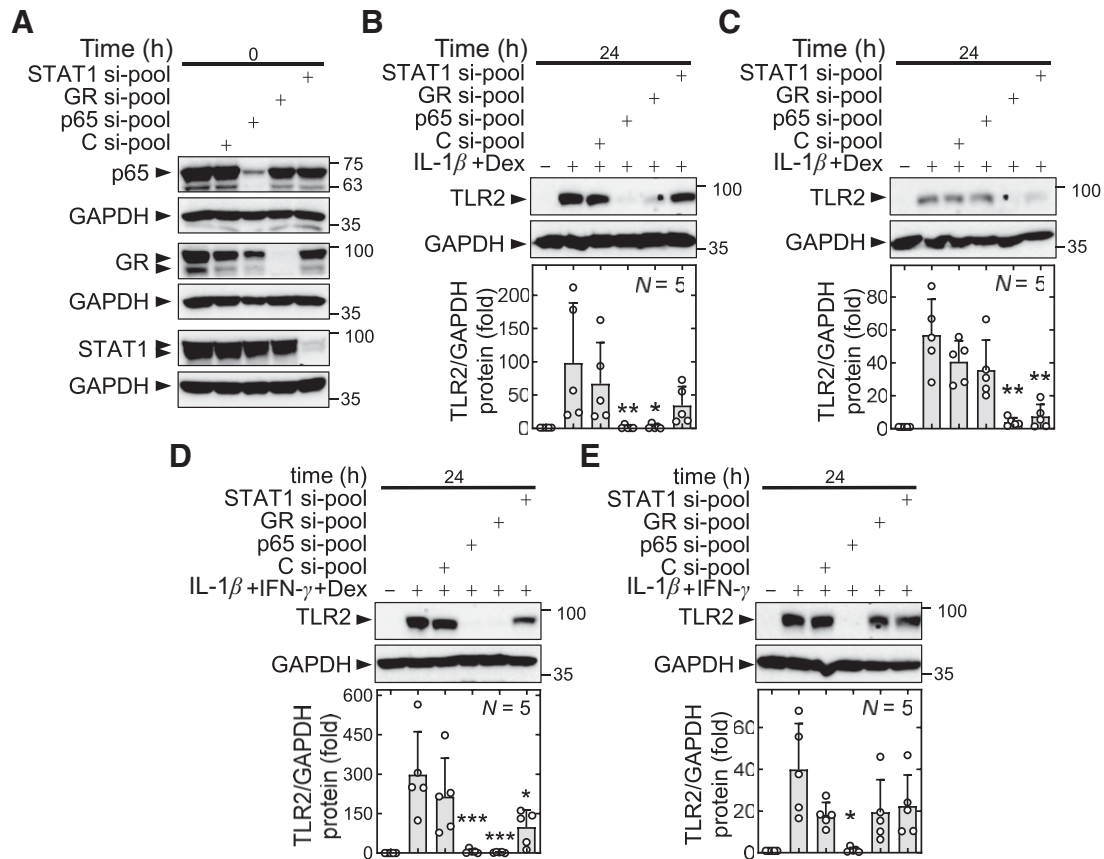


**Fig. 9.** Effect of p65, GR, and STAT1 knockdown on IL-1 $\beta$ , IFN- $\gamma$ , and dexamethasone-induced TLR2 expression in A549 cells. (A) A549 cells were incubated with pools of either control siRNAs (C si-pool), p65 siRNAs (p65 si-pool), GR siRNAs (GR si-pool), or STAT1 siRNAs (STAT1 si-pool) (1 nM each) for 48 hours. Cells were then incubated overnight with serum-free media prior to harvesting for western blot analysis. Representative blots of p65, GR, STAT1, and GAPDH from five independent experiments are shown. (B–E) A549 cells were incubated with siRNA pools as in (A), followed by treatment with IL-1 $\beta$  (1 ng/ml), IFN- $\gamma$  (10 ng/ml), and/or Dex (1  $\mu$ M), as indicated, for 24 hours. Cells were harvested for western blot analysis. Representative blots of TLR2 and GAPDH from *N* independent experiments are shown. Densitometric data were normalized to GAPDH, expressed as fold of untreated, and mean  $\pm$  S.D. were plotted as bar graphs overlaid with scatter plots. Significance relative to C si-pool in each case was tested using ANOVA with a Dunnett's post hoc test. \* $P \leq 0.05$ ; \*\* $P \leq 0.01$ ; \*\*\* $P \leq 0.001$ .

various combinations of IL-1 $\beta$ , IFN- $\gamma$ , and dexamethasone for 24 hours. With IL-1 $\beta$ +Dex, the control and STAT1-targeting siRNAs had no marked effect on TLR2 protein, whereas marked reductions ( $P \leq 0.01$  and  $0.05$ , respectively) in TLR2 protein were observed following knockdown of either p65 and/or GR (Fig. 9, A and B). This confirms roles for both p65 and GR in the induction of TLR2 expression by IL-1 $\beta$ +Dex. Likewise, in cells treated with IFN- $\gamma$ +Dex, the knockdown of STAT1 and GR reduced (both  $P \leq 0.01$ ) TLR2 protein levels, whereas control and p65 siRNA pools had no effect (Fig. 9, A and C). Therefore, STAT1 and GR appear to be involved in IFN- $\gamma$ +Dex-induced TLR2 expression. Similarly, in cells treated with the combination of IL-1 $\beta$ +IFN- $\gamma$ +Dex, whereas nontargeting control siRNAs had no significant effect, the p65 and GR siRNA pools almost completely abolished (both  $P \leq 0.001$ ) the IL-1 $\beta$ +IFN- $\gamma$ +Dex-induced TLR2 protein (Fig. 9D). The STAT1 siRNA pool also significantly ( $P \leq 0.05$ ), but only partially, reduced TLR2 expression induced by IL-1 $\beta$ +IFN- $\gamma$ +Dex (Fig. 9 D). These data confirm roles for p65, GR, and STAT1 in the induction of TLR2 expression by IL-1 $\beta$ , IFN- $\gamma$ , and dexamethasone in combination. Finally, in the case of IL-1 $\beta$ +IFN- $\gamma$ -treated A549 cells, only the p65 siRNA pool reduced ( $P \leq 0.05$ ) TLR2 protein, whereas the controls, GR, and STAT1-targeting siRNAs had no

effect on TLR2 expression (Fig. 9, A and E). This suggests that p65, but not STAT1, appears to be involved in the TLR2 expression induced by IL-1 $\beta$ +IFN- $\gamma$ .

## Discussion

Glucocorticoids have complex impacts on inflammation and variously downregulate or enhance gene expression (Busillo and Cidlowski, 2013; Cruz-Topete and Cidlowski, 2015; Amrani et al., 2020). Aside from metabolic effects, many glucocorticoid-enhanced genes, by controlling signaling and gene expression, are regulatory, whereas others are proinflammatory (Busillo et al., 2011; Newton et al., 2017). Mechanisms and relevance for these different effects remain poorly understood but are required to build a more comprehensive understanding of glucocorticoid action that considers both anti-inflammatory effects with potential enhancements of inflammatory responses. The current study focused on synergy between glucocorticoid and cytokines to induce TLR2 expression in human pulmonary epithelial cells. Consistent with prior reports, dexamethasone when combined with each of IL-1 $\beta$  or IFN- $\gamma$  supra-additively enhanced TLR2 expression in A549 cells (Shuto et al., 2002; Hermoso et al., 2004; Homma et al., 2004; Sakai et al., 2004; Hoppstädter et al., 2019; Bansal et al., 2022). Building from

this, we report that in A549 cells and pHBEs, a clear three-way *supra*-additivity occurred between the glucocorticoid, IL-1 $\beta$ , and IFN- $\gamma$  as a triple combination. At the mRNA level, the effect of this triple combination surpassed the responses to the individual and dual treatments. Indeed, occurring at maximally effective concentrations of each stimulus, this represents synergy between the three pathways that was readily apparent and replicated at both the mRNA and protein levels of TLR2 expression. Since all the current analyses were at 24 hours or less, further synergy could be observed at longer times, but this would require additional testing. Furthermore, replication of these effects in pHBEs grown in submersion culture supports A549 cells as a model for mechanistic investigations. Nevertheless, although pHBEs grown in ALI culture showed *supra*-additivity between IL-1 $\beta$  and glucocorticoid on TLR2 mRNA, effects of IFN- $\gamma$  were not apparent. This discrepancy could be due to several reasons. For example, IL-1 $\beta$  plus glucocorticoid may induce maximal TLR2 expression such that combinatorial effects with IFN- $\gamma$  require lower levels of IL-1 $\beta$  plus glucocorticoid stimulation. Moreover, signaling and the accessibility of regulatory elements responsible for TLR2 expression induced by IL-1 $\beta$ , IFN- $\gamma$ , and glucocorticoid may differ between undifferentiated pHBEs in submersion culture and highly differentiated ALI cultures. Equally, disparities in the expression of necessary factors between undifferentiated and differentiated pHBEs could differentially regulate TLR2, whereas enhancer usage can certainly change with differentiation state (Natoli, 2010). In addition, differential contributions by the various differentiated ALI cell types may confound the overall effect. Although not explored, this differential responsiveness could be relevant to heighten host responses in damaged pseudostratified epithelia, where cells undergo dedifferentiation as a necessary part of healing and restoration of barrier function.

To better understand combinatorial effects between glucocorticoid, IL-1 $\beta$ , and IFN- $\gamma$ , we identified key factors involved with each stimulus. The regulation of gene expression by IL-1 $\beta$  and IFN- $\gamma$  commonly involves NF- $\kappa$ B and STAT1, respectively (Pahl, 1999; Schroder et al., 2004), and can produce profound transcriptional synergy (Hiroi and Ohmori, 2005). However, such synergy was not readily observed for TLR2. Rather, TLR2 synergies required the presence of glucocorticoid, prompting us to explore roles for NF- $\kappa$ B, STAT1, and GR. The two glucocorticoids, dexamethasone and budesonide, used in the current study are both GR selective and produce synonymous effects on gene expression (Hellal-Levy et al., 1999; Millan et al., 2011; Mostafa et al., 2019). By employing Org34517, a competitive GR antagonist, that, unlike RU496 (mifepristone) (Jewell et al., 1995; Chivers et al., 2004; Rider et al., 2018), may not lead to GR translocation (Peeters et al., 2008) and which shows a much-reduced level of partial agonism (Joshi et al., 2015a,b), we indicate a role for GR. Given possible off-target effects of antagonists on other nuclear hormone receptors, we also used silencing of GR to provide compelling evidence for GR involvement in the synergy between IL-1 $\beta$ , IFN- $\gamma$ , and glucocorticoid. This aligns with glucocorticoid-induced GR binding to GRE-containing DNA regions upstream of human *TLR2* to activate transcription (Bansal et al., 2022).

The NF- $\kappa$ B pathway was explored using maximally effective concentrations of the IKK2-selective inhibitors PS-1145, ML120B, and TPCA-1. Partial, but significant, reductions in

IL-1 $\beta$ +IFN- $\gamma$ +Dex-induced TLR2 expression by PS-1145 and ML120B, as well as the near complete inhibition by TPCA-1, support roles for the IKK2-NF- $\kappa$ B pathway. However, the partial effects of PS-1145 and ML120B, combined with their greater selectivity for IKK2 compared with TPCA-1 (Gamble et al., 2012), also raise the possible involvement of non-IKK2 pathways. Conversely, the greater inhibition of NF- $\kappa$ B-dependent transcription and TLR2 expression observed for TPCA-1 compared with PS-1145 and ML120B implies off-target effects for this compound. Indeed, reports that TPCA-1 prevents IFN- $\gamma$ -induced responses, in the absence of NF- $\kappa$ B activation, support this concern (Tudhope et al., 2007). Nevertheless, following p65 silencing, the resultant loss of TLR2 expression when induced by IL-1 $\beta$ +IFN- $\gamma$ +Dex, but not by IFN- $\gamma$ +Dex, indicates a key role for NF- $\kappa$ B. Given p65 binding to the human *TLR2* promoter (Bansal et al., 2022), the current data confirms p65/NF- $\kappa$ B in synergy between IL-1 $\beta$ , IFN- $\gamma$ , and glucocorticoid.

IFN- $\gamma$  treatment of A549 cells induced STAT1 phosphorylation at S727 and Y701, with Y701 phosphorylation markedly preceding that for S727. Although consistent with STAT1 activation (Wen et al., 1995; Sadzak et al., 2008), the delay in S727 phosphorylation compared with the rapid increase in Y701 phosphorylation suggests mechanistic differences. It is likely that IFN- $\gamma$  receptor activation produces rapid JAK-dependent phosphorylation of Y701, facilitating STAT1 nuclear localization (Sadzak et al., 2008). Conversely, delayed S727 phosphorylation may involve an independent pathway or be consequent on prior Y701 phosphorylation. Notably, S727 phosphorylation was induced by IL-1 $\beta$ , and additive summation with the effect of IFN- $\gamma$  suggests additional, likely non-JAK, pathways to phosphorylate S727. Indeed, mitogen activated protein kinases (MAPKs), which are activated by IL-1 $\beta$  in these cells (Shah et al., 2014), can phosphorylate S727 (Kovarik et al., 1999; Ramsauer et al., 2002; Zhang et al., 2004). However, in considering effects of IL-1 $\beta$  on S727 phosphorylation, it is salient that IFN- $\gamma$ -induced STAT1/GAS reporter activity was reduced upon cotreatment with IL-1 $\beta$  and therefore questions a positive role for this phosphorylation event.

Although the JAK inhibitors AZD1480, baricitinib, and ruxolitinib were highly efficacious and similarly potent on IFN- $\gamma$ -induced STAT1 reporter activity, their effects on STAT1 phosphorylation suggest site-specific differences. Specifically, S727 phosphorylation, compared with Y701 phosphorylation, appeared more sensitive to inhibition by AZD1480 and baricitinib relative to ruxolitinib. Various possibilities may explain this. Given the time lag between Y701 and S727 phosphorylation, it is possible that high levels of JAK activity are required for subsequent S727 phosphorylation. Therefore, modest inhibition of the relevant JAK could reduce S727 phosphorylation while having a reduced or no effect on Y701 phosphorylation. However, this hypothesis predicts parallel inhibitory effects of each inhibitor on each phosphorylation. This was likely not observed for ruxolitinib, and this raises the possibility that the differential selectivity of the inhibitors for JAK1, JAK2, JAK3, and Tyk2 could explain the data. Indeed, AZD1480 and baricitinib are relatively selective for JAK1 and JAK2, whereas ruxolitinib shows a less selective inhibition profile against the four JAKs (Fridman et al., 2010; Quintás-Cardama et al., 2010; Ioannidis et al., 2011). Therefore, different JAKs may plausibly produce these two phosphorylation events. This will need to be resolved by

additional studies. Further, all three compounds revealed similar, but lower, potency on the STAT1 reporter. Thus, although STAT1 phosphorylation was relatively sensitive to JAK inhibition, the reporter system may show a “reserve” requiring higher levels of kinase inhibition to reduce reporter activity. This is consistent with the silencing of STAT1, where >90% loss of STAT1 protein produced just over 50% inhibition of reporter activity. Similar effects on other pathways involving kinase activation of transcriptional responses are observed, which, anecdotally, aligns with signal amplification and signaling reserves toward the distal parts of pathways.

Regarding synergies produced by IL-1 $\beta$ , IFN- $\gamma$ , and glucocorticoid on TLR2 expression, we provide strong evidence for roles of pathways leading to NF- $\kappa$ B, STAT1, and GR. However, coactivation of these pathways had little effect on transcriptional activation produced by each factor acting via its respective consensus motif. This necessitates gene-specific explanations for the observed synergy. In prior studies, GR and p65 binding to upstream regions of the *TLR2* locus was unaffected by cotreatments and suggested that the presence of both factors at the *TLR2* promoter was sufficient for combinatorial effects (Bansal et al., 2022). However, these same promoter regions were unresponsive to IFN- $\gamma$  (data not shown), indicating involvement of STAT1 at distinct genomic regions. Further studies are therefore required to delineate any such regions.

The current findings advance understanding of the mechanisms leading to synergy but do not address the functional significance of TLR2 synergy. Prior investigators have debated pro- and anti-inflammatory effects for TLR2 (Imasato et al., 2002; Homma et al., 2004; Winder et al., 2009; Hoppstädter et al., 2019). However, TLR2 agonism in cells showing IL-1 $\beta$ +Dex-induced TLR2 stimulated NF- $\kappa$ B reporter activity and induced CXCL8 and CCL5 expression (Bansal et al., 2022). This is consistent with other TLR and IL1 family receptors, which activate NF- $\kappa$ B, MAPKs, and inflammatory responses (O'Neill and Bowie, 2007). Likewise, in pHBECS treated with TNF or IFN- $\gamma$  plus dexamethasone, TLR2 agonists induce expression of inflammatory genes that include IL6, CXCL8, and human  $\beta$ -defensin-2 (Hertz et al., 2003; Homma et al., 2004; Winder et al., 2009). Moreover, as TLR2 agonism reduced responsiveness to  $\beta_2$  agonists and glucocorticoids (Alkhoury et al., 2014; Rahman et al., 2016), its expression may be unhelpful in chronic inflammatory diseases. Indeed, TLR2 expression is widely documented as being elevated in severe asthma (Simpson et al., 2007; Singhania et al., 2018; Zhang et al., 2021), a condition in which patients are subjected to high-intensity therapies involving  $\beta_2$ -adrenoceptor agonists and glucocorticoids. Conversely, enhanced TLR2 expression and activation of inflammatory responses may facilitate host defense responses, while glucocorticoids simultaneously suppress general inflammation and promote healing (Busillo and Cidlowksi, 2013; Cruz-Topete and Cidlowksi, 2015; Amrani et al., 2020). Thus, the cooperation between GR, NF- $\kappa$ B, and STAT1 to induce TLR2 expression may be important for normal host defense but could be undesirable in the (glucocorticoid) treatment of chronic inflammatory disease, including severe asthma, where the expression of cytokines such as IL-1 $\beta$  and IFN- $\gamma$  is expected. Indeed, although priming of the innate immune response is reported for

TLR2 agonists and may be enhanced in the presence of glucocorticoid (Alshaghдали et al., 2021; Deliyannis et al., 2021; Girkin et al., 2021), the antagonism of TLR2, or targeting of TLRs, has also been shown to reduce expression of inflammatory mediators (Su and Weindl, 2018; Thapa et al., 2023).

#### Acknowledgments

The authors would like to thank David Proud for his assistance with the provision of pHBECS. They also would like to acknowledge the Canadian Fund of Innovation (CFI) and the Alberta Science and Research Authority for providing an equipment and infrastructure grant to perform real-time PCR.

#### Data Availability

This article contains no datasets generated or analyzed during the current study.

#### Authorship Contributions

*Participated in research design:* Bansal, Newton.

*Conducted experiments:* Bansal, Kooi, Kalyanaraman, Gill, Thorne, Chandramohan, Necker-Brown, Mostafa, Milani.

*Contributed new reagents or analytical tools:* Leigh, Newton.

*Performed data analysis:* Bansal, Kooi, Kalyanaraman, Gill, Thorne, Chandramohan, Necker-Brown, Mostafa, Milani.

*Wrote or contributed to the writing of the manuscript:* Bansal, Leigh, Newton.

#### References

- Akira S, Takeda K, and Kaisho T (2001) Toll-like receptors: critical proteins linking innate and acquired immunity. *Nat Immunol* **2**:675–680.
- Alkhoury H, Rumzum NN, Rahman MM, FitzPatrick M, de Pedro M, Oliver BG, Bourke JE, and Ammit AJ (2014) TLR2 activation causes tachyphylaxis to  $\beta_2$  agonists in vitro and ex vivo: modelling bacterial exacerbation. *Allergy* **69**:1215–1222.
- Alshaghдали K, Saeed M, Kamal MA, and Saeed A (2021) Interaction of Ectodomain of Respiratory Syncytial Virus G Protein with TLR2/TLR6 Heterodimer: An In vitro and In silico Approach to Decipher the Role of RSV G Protein in Pro-inflammatory Response against the Virus. *Curr Pharm Des* **27**:4464–4476.
- Altonsy MO, Sasse SK, Phang TL, and Gerber AN (2014) Context-dependent cooperation between nuclear factor  $\kappa$ B (NF- $\kappa$ B) and the glucocorticoid receptor at a TNFAIP3 intronic enhancer: a mechanism to maintain negative feedback control of inflammation. *J Biol Chem* **289**:8231–8239.
- Amrani Y, Panettieri RA, Ramos-Ramirez P, Schaafsma D, Kaczmarek K, and Thliba O (2020) Important lessons learned from studies on the pharmacology of glucocorticoids in human airway smooth muscle cells: Too much of a good thing may be a problem. *Pharmacol Ther* **213**:107589.
- Bansal A, Mostafa MM, Kooi C, Sasse SK, Michi AN, Shah SV, Leigh R, Gerber AN, and Newton R (2022) Interplay between nuclear factor- $\kappa$ B, p38 MAPK, and glucocorticoid receptor signaling synergistically induces functional TLR2 in lung epithelial cells. *J Biol Chem* **298**:101747.
- Barnes PJ (2013) New anti-inflammatory targets for chronic obstructive pulmonary disease. *Nat Rev Drug Discov* **12**:543–559.
- Britt Jr RD, Thompson MA, Sasse S, Pabelick CM, Gerber AN, and Prakash YS (2019) Th1 cytokines TNF- $\alpha$  and IFN- $\gamma$  promote corticosteroid resistance in developing human airway smooth muscle. *Am J Physiol Lung Cell Mol Physiol* **316**:L71–L81.
- Busillo JM, Azzam KM, and Cidlowksi JA (2011) Glucocorticoids sensitize the innate immune system through regulation of the NLRP3 inflammasome. *J Biol Chem* **286**:38703–38713.
- Busillo JM and Cidlowksi JA (2013) The five Rs of glucocorticoid action during inflammation: ready, reinforce, repress, resolve, and restore. *Trends Endocrinol Metab* **24**:109–119.
- Catley MC, Cambridge LM, Nasuhara Y, Ito K, Chivers JE, Beaton A, Holden NS, Bergmann MW, Barnes PJ, and Newton R (2004) Inhibitors of protein kinase C (PKC) prevent activated transcription: role of events downstream of NF-kappaB DNA binding. *J Biol Chem* **279**:18457–18466.
- Chivers JE, Cambridge LM, Catley MC, Mak JC, Donnelly LE, Barnes PJ, and Newton R (2004) Differential effects of RU486 reveal distinct mechanisms for glucocorticoid repression of prostaglandin E release. *Eur J Biochem* **271**:4042–4052.
- Cruz-Topete D and Cidlowksi JA (2015) One hormone, two actions: anti- and pro-inflammatory effects of glucocorticoids. *Neuroimmunomodulation* **22**:20–32.
- De Bosscher K and Haegeman G (2009) Minireview: latest perspectives on anti-inflammatory actions of glucocorticoids. *Mol Endocrinol* **23**:281–291.
- Decker T, Kovarik P, and Meinke A (1997) GAS elements: a few nucleotides with a major impact on cytokine-induced gene expression. *J Interferon Cytokine Res* **17**:121–134.

- Deliyannis G, Wong CY, McQuilten HA, Bachem A, Clarke M, Jia X, Horrocks K, Zeng W, Girkin J, Scott NE, et al. (2021) TLR2-mediated activation of innate responses in the upper airways confers antiviral protection of the lungs. *JCI Insight* **6**:e140267.
- Fridman JS, Scherle PA, Collins R, Burn TC, Li Y, Li J, Covington MB, Thomas B, Collier P, Favata MF, et al. (2010) Selective inhibition of JAK1 and JAK2 is efficacious in rodent models of arthritis: preclinical characterization of INCB028050. *J Immunol* **184**:5298–5307.
- Gamble C, McIntosh K, Scott R, Ho KH, Plevin R, and Paul A (2012) Inhibitory kappa B Kinases as targets for pharmacological regulation. *Br J Pharmacol* **165**:802–819.
- Girkin J, Loo S-L, Esneau C, Maltby S, Mercuri F, Chua B, Reid AT, Veerati PC, Grainge CL, Wark PAB, et al. (2021) TLR2-mediated innate immune priming boosts lung anti-viral immunity. *Eur Respir J* **58**:2001584.
- Hellal-Levy C, Couette B, Fagart J, Souque A, Gomez-Sanchez C, and Rafestin-Oblin M (1999) Specific hydroxylations determine selective corticosteroid recognition by human glucocorticoid and mineralocorticoid receptors. *FEBS Lett* **464**:9–13.
- Hermoso MA, Matsuguchi T, Smoak K, and Cidlowski JA (2004) Glucocorticoids and tumor necrosis factor alpha cooperatively regulate toll-like receptor 2 gene expression. *Mol Cell Biol* **24**:4743–4756.
- Hertz CJ, Wu Q, Porter EM, Zhang YJ, Weismüller K-H, Godowski PJ, Ganz T, Randell SH, and Modlin RL (2003) Activation of Toll-like receptor 2 on human tracheobronchial epithelial cells induces the antimicrobial peptide human  $\beta$  defensin-2. *J Immunol* **171**:6820–6826.
- Hiroi M and Ohmori Y (2005) Transcriptional Synergism between NF- $\kappa$ B and STAT1. *J Oral Biosci* **47**:230–242.
- Hofmann TG and Schmitz ML (2002) The promoter context determines mutual repression or synergism between NF- $\kappa$ B and the glucocorticoid receptor. *Biol Chem* **383**:1947–1951.
- Homma T, Kato A, Hashimoto N, Batchelor J, Yoshikawa M, Imai S, Wakiguchi H, Saito H, and Matsumoto K (2004) Corticosteroid and cytokines synergistically enhance toll-like receptor 2 expression in respiratory epithelial cells. *Am J Respir Cell Mol Biol* **31**:463–469.
- Hoppstädter J, Dembek A, Linnenberger R, Dahlem C, Barghash A, Fecher-Trost C, Fuhrmann G, Koch M, Kraegeloh A, Huwer H, et al. (2019) Toll-Like Receptor 2 Release by Macrophages: An Anti-inflammatory Program Induced by Glucocorticoids and Lipopolysaccharide. *Front Immunol* **10**:1634.
- Hudy MH, Traves SL, Wiehler S, and Proud D (2010) Cigarette smoke modulates rhinovirus-induced airway epithelial cell chemokine production. *Eur Respir J* **35**:1256–1263.
- Imai E, Stromstedt PE, Quinn PG, Carlstedt-Duke J, Gustafsson JA, and Granner DK (1990) Characterization of a complex glucocorticoid response unit in the phosphoenolpyruvate carboxykinase gene. *Mol Cell Biol* **10**:4712–4719.
- Imasato A, Desbois-Mouthon C, Han J, Kai H, Cato ACB, Akira S, and Li JD (2002) Inhibition of p38 MAPK by glucocorticoids via induction of MAPK phosphatase-1 enhances nontypeable Haemophilus influenzae-induced expression of toll-like receptor 2. *J Biol Chem* **277**:47444–47450.
- Ioannidis S, Lamb ML, Wang T, Almeida L, Block MH, Davies AM, Peng B, Su M, Zhang H-J, Hoffmann E, et al. (2011) Discovery of 5-chloro-N<sub>2</sub>-(1S)-1-(5-fluoropyrimidin-2-yl)ethyl-N<sub>4</sub>-(5-methyl-1H-pyrazol-3-yl)pyrimidine-2,4-diamine (AZD1480) as a novel inhibitor of the Jak/Stat pathway. *J Med Chem* **54**:262–276.
- Jantzen HM, Strähle U, Gloss B, Stewart F, Schmid W, Boshart M, Miksicki R, and Schütz G (1987) Cooperativity of glucocorticoid response elements located far upstream of the tyrosine aminotransferase gene. *Cell* **49**:29–38.
- Jewell CM, Webster JC, Burnstein KL, Sar M, Bodwell JE, and Cidlowski JA (1995) Immunocytochemical analysis of hormone mediated nuclear translocation of wild type and mutant glucocorticoid receptors. *J Steroid Biochem Mol Biol* **55**:135–146.
- Joshi T, Johnson M, Newton R, and Giembycz M (2015a) An analysis of glucocorticoid receptor-mediated gene expression in BEAS-2B human airway epithelial cells identifies distinct, ligand-directed, transcription profiles with implications for asthma therapeutics. *Br J Pharmacol* **172**:1360–1378.
- Joshi T, Johnson M, Newton R, and Giembycz MA (2015b) The long-acting  $\beta$ 2-adrenoceptor agonist, indacaterol, enhances glucocorticoid receptor-mediated transcription in human airway epithelial cells in a gene- and agonist-dependent manner. *Br J Pharmacol* **172**:2634–2653.
- Kelly MM, King EM, Rider CF, Gwozd C, Holden NS, Eddleston J, Zuraw B, Leigh R, O'Byrne PM, and Newton R (2012) Corticosteroid-induced gene expression in allergen-challenged asthmatic subjects taking inhaled budesonide. *Br J Pharmacol* **165**:1737–1747.
- King EM, Holden NS, Gong W, Rider CF, and Newton R (2009) Inhibition of NF- $\kappa$ B-dependent transcription by MKP-1: transcriptional repression by glucocorticoids occurring via p38 MAPK. *J Biol Chem* **284**:26803–26815.
- Klaßen C, Karabinskaya A, Dejager L, Vettorazzi S, Van Moorleghem J, Lühder F, Meijising SH, Tuckermann JP, Bohnenberger H, Libert C, et al. (2017) Airway Epithelial Cells Are Crucial Targets of Glucocorticoids in a Mouse Model of Allergic Asthma. *J Immunol* **199**:48–61.
- Kovarik P, Stoiber D, Eyers PA, Menghini R, Neiningner A, Gaestel M, Cohen P, and Decker T (1999) Stress-induced phosphorylation of STAT1 at Ser727 requires p38 mitogen-activated protein kinase whereas IFN- $\gamma$  uses a different signaling pathway. *Proc Natl Acad Sci USA* **96**:13956–13961.
- Lambrecht BN and Hammad H (2012) The airway epithelium in asthma. *Nat Med* **18**:684–692.
- Lambrecht BN, Hammad H, and Fahy JV (2019) The Cytokines of Asthma. *Immunity* **50**:975–991.
- Liu D, Ahmet A, Ward L, Krishnamoorthy P, Mandelcorn ED, Leigh R, Brown JP, Cohen A, and Kim H (2013) A practical guide to the monitoring and management of the complications of systemic corticosteroid therapy. *Allergy Asthma Clin Immunol* **9**:30.
- Michi AN and Proud D (2021) A toolbox for studying respiratory viral infections using air-liquid interface cultures of human airway epithelial cells. *Am J Physiol Lung Cell Mol Physiol* **321**:L263–L280.
- Millan DS, Ballard SA, Chunn S, Dybowski JA, Fulton CK, Glossop PA, Guillabert E, Hewson CA, Jones RM, Lamb DJ, et al. (2011) Design and synthesis of long acting inhaled corticosteroids for the treatment of asthma. *Bioorg Med Chem Lett* **21**:5826–5830.
- Miyata M, Lee J-Y, Susuki-Miyata S, Wang WY, Xu H, Kai H, Kobayashi KS, Flavell RA, and Li J-D (2015) Glucocorticoids suppress inflammation via the upregulation of negative regulator IRAK-M. *Nat Commun* **6**:6062.
- Mostafa MM, Rider CF, Shah S, Traves SL, Gordon PMK, Miller-Larsson A, Leigh R, and Newton R (2019) Glucocorticoid-driven transcriptomes in human airway epithelial cells: commonalities, differences and functional insight from cell lines and primary cells. *BMC Med Genomics* **12**:29.
- Natoli G (2010) Maintaining cell identity through global control of genomic organization. *Immunity* **33**:12–24.
- Newton R, Adcock IM, and Barnes PJ (1996) Superinduction of NF- $\kappa$ B by actinomycin D and cycloheximide in epithelial cells. *Biochem Biophys Res Commun* **218**:518–523.
- Newton R, Hart LA, Stevens DA, Bergmann M, Donnelly LE, Adcock IM, and Barnes PJ (1998) Effect of dexamethasone on interleukin-1 $\beta$ -(IL-1 $\beta$ )-induced nuclear factor-kappaB (NF-kappaB) and kappaB-dependent transcription in epithelial cells. *Eur J Biochem* **254**:81–89.
- Newton R and Holden NS (2007) Separating transrepression and transactivation: a distressing divorce for the glucocorticoid receptor? *Mol Pharmacol* **72**:799–809.
- Newton R, Shah S, Altomonte MO, and Gerber AN (2017) Glucocorticoid and cytokine crosstalk: Feedback, feedforward, and co-regulatory interactions determine repression or resistance. *J Biol Chem* **292**:7163–7172.
- Ngoc PL, Gold DR, Tzianabos AO, Weiss ST, and Celedón JC (2005) Cytokines, allergy, and asthma [published correction appears in *Curr Opin Allergy Clin Immunol* (2005) 5:307]. *Curr Opin Allergy Clin Immunol* **5**:161–166.
- O'Neill LAJ and Bowie AG (2007) The family of five: TIR-domain-containing adaptors in Toll-like receptor signalling. *Nat Rev Immunol* **7**:353–364.
- Oh KS, Patel H, Gottschalk RA, Lee WS, Baek S, Fraser IDC, Hager GL, and Sung MH (2017) Anti-Inflammatory Chromatin Landscape Suggests Alternative Mechanisms of Glucocorticoid Receptor Action. *Immunity* **47**:298–309.
- Pahl HL (1999) Activators and target genes of Rel/NF- $\kappa$ B transcription factors. *Oncogene* **18**:6853–6866.
- Peeters BWMM, Ruijt GSF, Craighead M, and Kitchener P (2008) Differential effects of the new glucocorticoid receptor antagonist ORG 34517 and RU486 (mifepristone) on glucocorticoid receptor nuclear translocation in the AtT20 cell line. *Ann N Y Acad Sci* **1148**:536–541.
- Peeters BWMM, Tonnaer JADM, Groen MB, Broekkamp CLE, van der Voort HAA, Schoonen WGFJ, Smets RJM, Vanderheyden PML, Gebhard R, and Ruijt GSF (2004) Glucocorticoid receptor antagonists: new tools to investigate disorders characterized by cortisol hypersecretion. *Stress* **7**:233–241.
- Quintás-Cardama A, Vaddi K, Liu P, Manshourti T, Li J, Scherle PA, Caulder E, Wen X, Li Y, Waeltz P, et al. (2010) Preclinical characterization of the selective JAK1/2 inhibitor INCB018424: therapeutic implications for the treatment of myeloproliferative neoplasms. *Blood* **115**:3109–3117.
- Rahman MM, Prabhala P, Rumzhum NN, Patel BS, Wickop T, Hansbro PM, Verrills NM, and Ammit AJ (2016) TLR2 ligation induces corticosteroid insensitivity in A549 lung epithelial cells: Anti-inflammatory impact of PP2A activators. *Int J Biochem Cell Biol* **78**:279–287.
- Ramsauer K, Sadzak I, Porras A, Pilz A, Nebreda AR, Decker T, and Kovarik P (2002) p38 MAPK enhances STAT1-dependent transcription independently of Ser-727 phosphorylation. *Proc Natl Acad Sci USA* **99**:12859–12864.
- Rhen T and Cidlowski JA (2005) Antiinflammatory action of glucocorticoids—new mechanisms for old drugs. *N Engl J Med* **353**:1711–1723.
- Rider CF, Altomonte MO, Mostafa MM, Shah SV, Sasse S, Manson ML, Yan D, Kärrman-Märch C, Miller-Larsson A, Gerber AN, et al. (2018) Long-Acting  $\beta$ 2-Adrenoceptor Agonists Enhance Glucocorticoid Receptor (GR)-Mediated Transcription by Gene-Specific Mechanisms Rather Than Generic Effects via GR. *Mol Pharmacol* **94**:1031–1046.
- Rider CF, Shah S, Miller-Larsson A, Giembycz MA, and Newton R (2015) Cytokine-induced loss of glucocorticoid function: effect of kinase inhibitors, long-acting  $\beta$ (2)-adrenoceptor [corrected] agonist and glucocorticoid receptor ligands. *PLoS One* **10**:e0116773.
- Sadzak I, Schiff M, Gattermeier I, Glinitzer R, Sauer I, Saalmüller A, Yang E, Schaljo B, and Kovarik P (2008) Recruitment of Stat1 to chromatin is required for interferon-induced serine phosphorylation of Stat1 transactivation domain. *Proc Natl Acad Sci USA* **105**:8944–8949.
- Sakai A, Han J, Cato ACBB, Akira S, and Li J-DD (2004) Glucocorticoids synergize with IL-1 $\beta$  to induce TLR2 expression via MAP Kinase Phosphatase-1-dependent dual inhibition of MAPK JNK and p38 in epithelial cells. *BMC Mol Biol* **5**:2.
- Schroder K, Hertzog PJ, Ravasi T, and Hume DA (2004) Interferon- $\gamma$ : an overview of signals, mechanisms and functions. *J Leukoc Biol* **75**:163–189.
- Shah S, King EM, Chandrasekhar A, and Newton R (2014) Roles for the mitogen-activated protein kinase (MAPK) phosphatase, DUSP1, in feedback control of inflammatory gene expression and repression by dexamethasone. *J Biol Chem* **289**:13667–13679.
- Shuto T, Imasato A, Jono H, Sakai A, Xu H, Watanabe T, Rixter DD, Kai H, Andalibi A, Linthicum F, et al. (2002) Glucocorticoids synergistically enhance nontypeable Haemophilus influenzae-induced Toll-like receptor 2 expression via a negative cross-talk with p38 MAP kinase. *J Biol Chem* **277**:17263–17270.
- Simpson JL, Grissell TV, Douwes J, Scott RJ, Boyle MJ, and Gibson PG (2007) Innate immune activation in neutrophilic asthma and bronchiectasis. *Thorax* **62**:211–218.
- Singhania A, Wallington JC, Smith CG, Horowitz D, Staples KJ, Howarth PH, Gadola SD, Djukanović R, Woelck CH, and Hinks TSC (2018) Multitissue Transcriptomics Delineates the Diversity of Airway T Cell Functions in Asthma. *Am J Respir Cell Mol Biol* **58**:261–270.

- Su Q and Weindl G (2018) Glucocorticoids and Toll-like receptor 2 cooperatively induce acute-phase serum amyloid A. *Pharmacol Res* **128**:145–152.
- Tam A, Wadsworth S, Dorscheid D, Man SF, and Sin DD (2011) The airway epithelium: more than just a structural barrier. *Thor Adv Respir Dis* **5**:255–273.
- Thapa B, Pak S, Chung D, Shin HK, Lee SH, and Lee K (2023) Cell-penetrating TLR inhibitor peptide alleviates ulcerative colitis by the functional modulation of macrophages. *Front Immunol* **14**:1165667.
- Thorne A, Bansal A, Necker-Brown A, Mostafa MM, Gao A, Georgescu A, Kooi C, Leigh R, and Newton R (2023) Differential regulation of BIRC2 and BIRC3 expression by inflammatory cytokines and glucocorticoids in pulmonary epithelial cells. *PLoS One* **18**:e0286783.
- Tiba O, Damera G, Banerjee A, Gu S, Baidouri H, Keslacy S, and Amrani Y (2008) Cytokines induce an early steroid resistance in airway smooth muscle cells: novel role of interferon regulatory factor-1. *Am J Respir Cell Mol Biol* **38**:463–472.
- Tudhope SJ, Catley MC, Fenwick PS, Russell REK, Rumsey WL, Newton R, Barnes PJ, and Donnelly LE (2007) The role of IkappaB kinase 2, but not activation of NF-kappaB, in the release of CXCR3 ligands from IFN-gamma-stimulated human bronchial epithelial cells. *J Immunol* **179**:6237–6245.
- Warner SM, Wiehler S, Michi AN, and Proud D (2019) Rhinovirus replication and innate immunity in highly differentiated human airway epithelial cells. *Respir Res* **20**:150.
- Wen Z, Zhong Z, and Darnell Jr JE (1995) Maximal activation of transcription by Stat1 and Stat3 requires both tyrosine and serine phosphorylation. *Cell* **82**:241–250.
- Winder AA, Wohlford-Lenane C, Scheetz TE, Nardy BN, Manzel LJ, Look DC, and McCray Jr PB (2009) Differential effects of cytokines and corticosteroids on toll-like receptor 2 expression and activity in human airway epithelia. *Respir Res* **10**:96.
- Zhang Y, Cho YY, Petersen BL, Zhu F, and Dong Z (2004) Evidence of STAT1 phosphorylation modulated by MAPKs, MEK1 and MSK1. *Carcinogenesis* **25**:1165–1175.
- Zhang Z, Wang J, and Chen O (2021) Identification of biomarkers and pathogenesis in severe asthma by coexpression network analysis. *BMC Med Genomics* **14**:51.

---

**Address correspondence to:** Dr. Robert Newton, HRIC-4C56, 3330 Hospital Drive NW, Calgary, Alberta, Canada T2N 4N1. E-mail: rnewton@ucalgary.ca

---



Journal Title: Molecular Pharmacology

Manuscript # MOLPHARM-AR-2023-000740

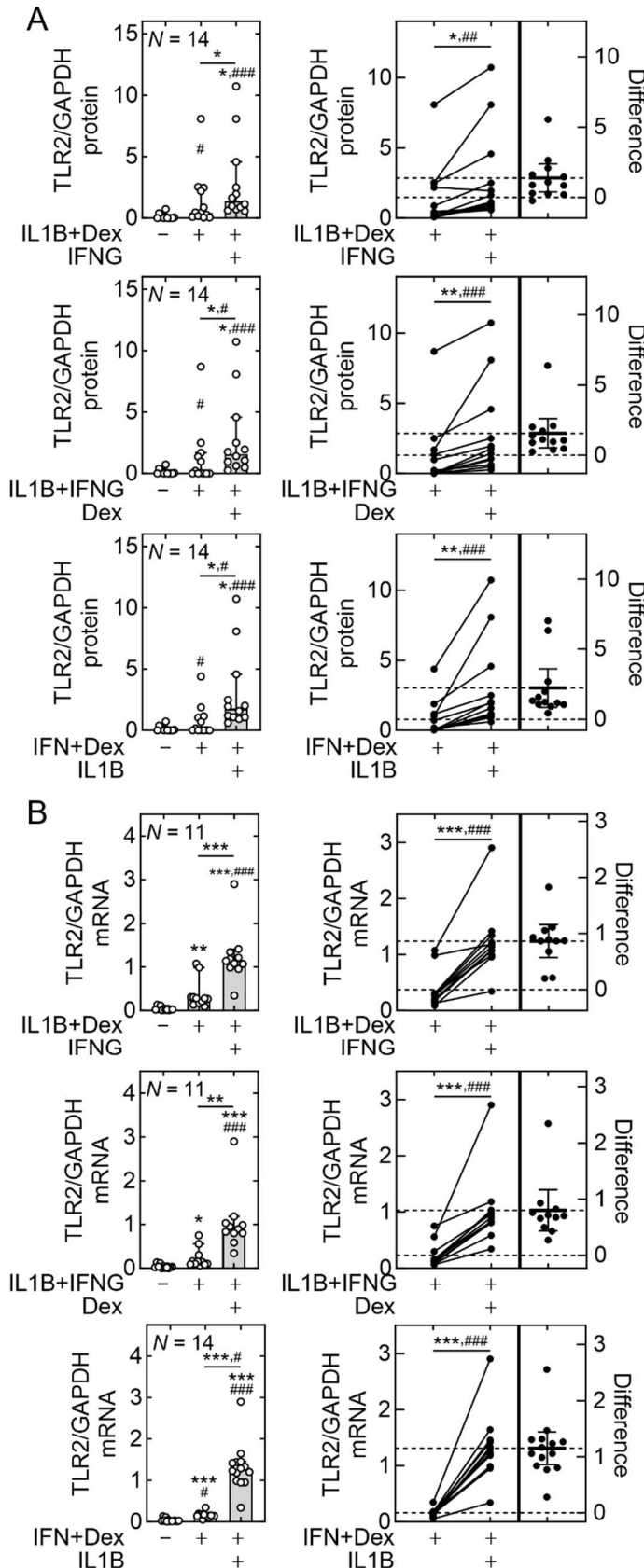
Supplemental data:

Synergy between interleukin-1 $\beta$ , interferon- $\gamma$  and glucocorticoids to induce TLR2 expression involves NF- $\kappa$ B, STAT1 and GR

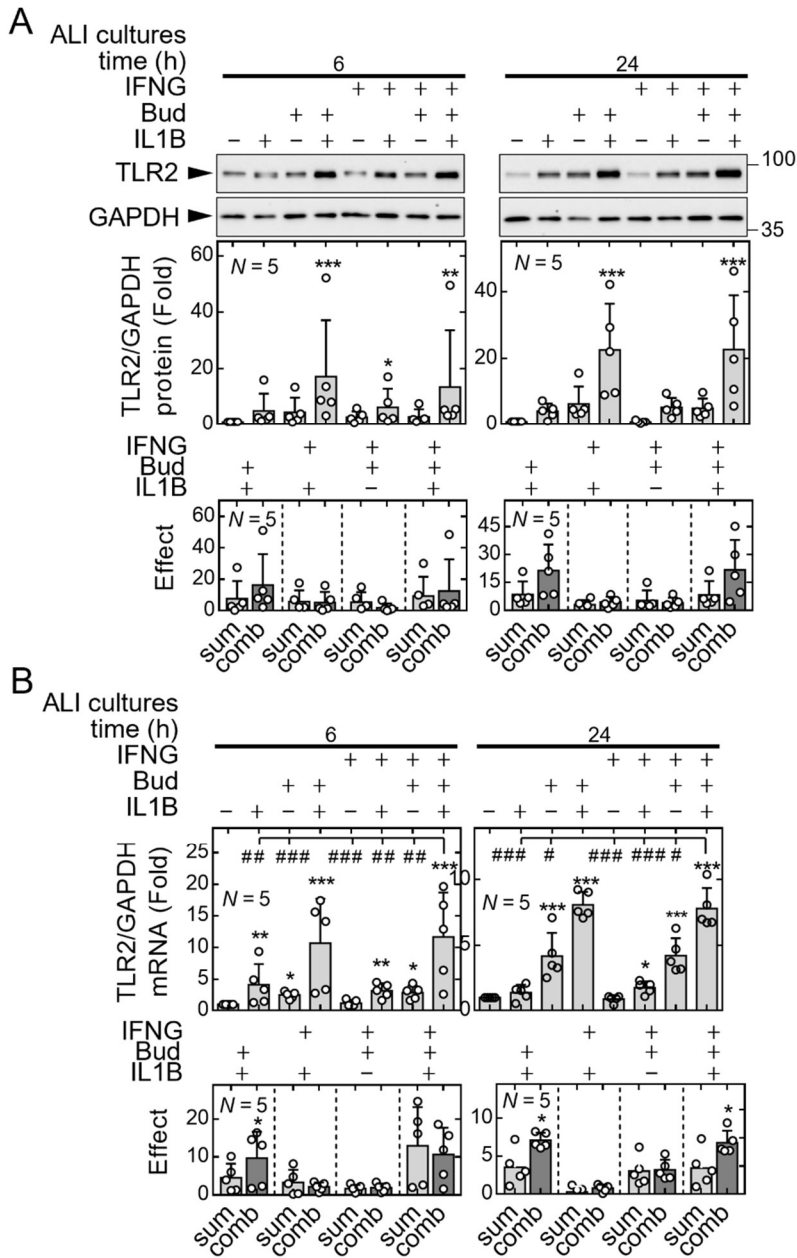
Akanksha Bansal<sup>1</sup>, Cora Kooi<sup>2</sup>, Keerthana Kalyanaraman<sup>1</sup>, Sachman Gill<sup>1</sup>, Andrew Thorne<sup>1</sup>, Priyanka Chandramohan<sup>1</sup>, Amandah Necker-Brown<sup>1</sup>, Mahmoud M. Mostafa<sup>1</sup>, Arya Milani<sup>1</sup>, Richard Leigh<sup>2</sup>, and Robert Newton<sup>1\*</sup>

**Affiliations:** <sup>1</sup>Department of Physiology & Pharmacology and <sup>2</sup>Department of Medicine, Lung Health Research Group, Snyder Institute for Chronic Diseases, Cumming School of Medicine, University of Calgary, AB, Canada.

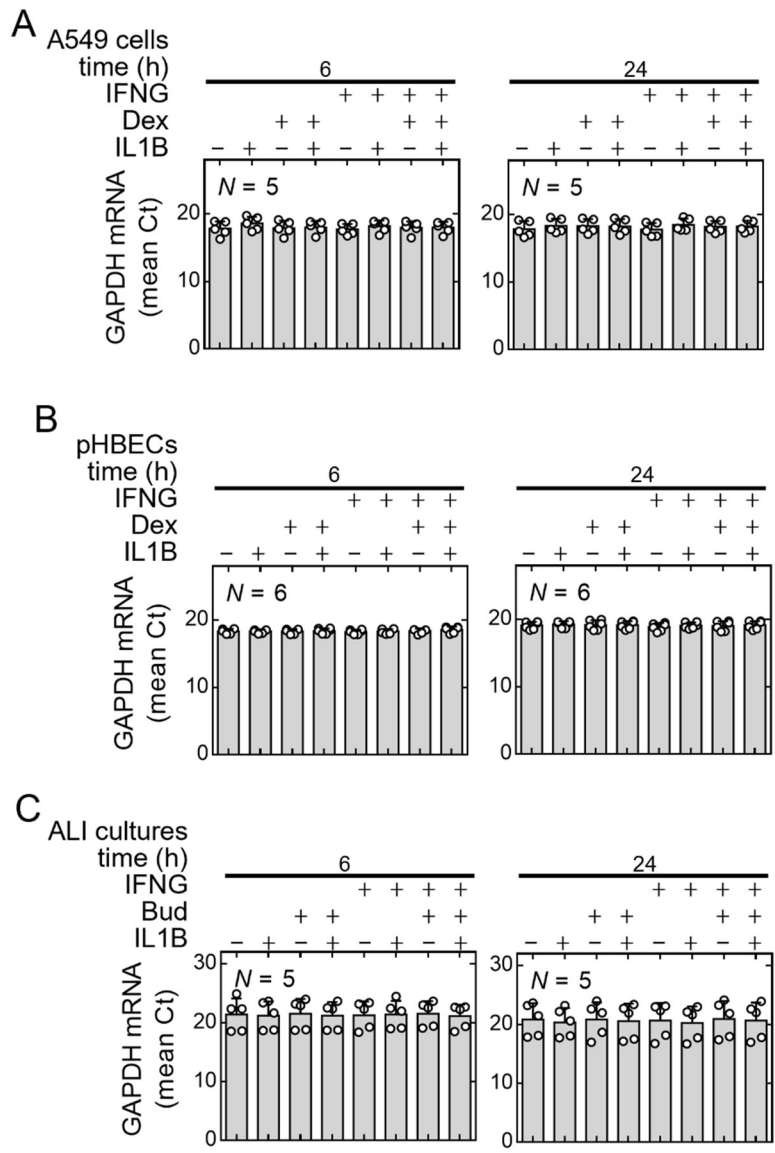
\*Corresponding author



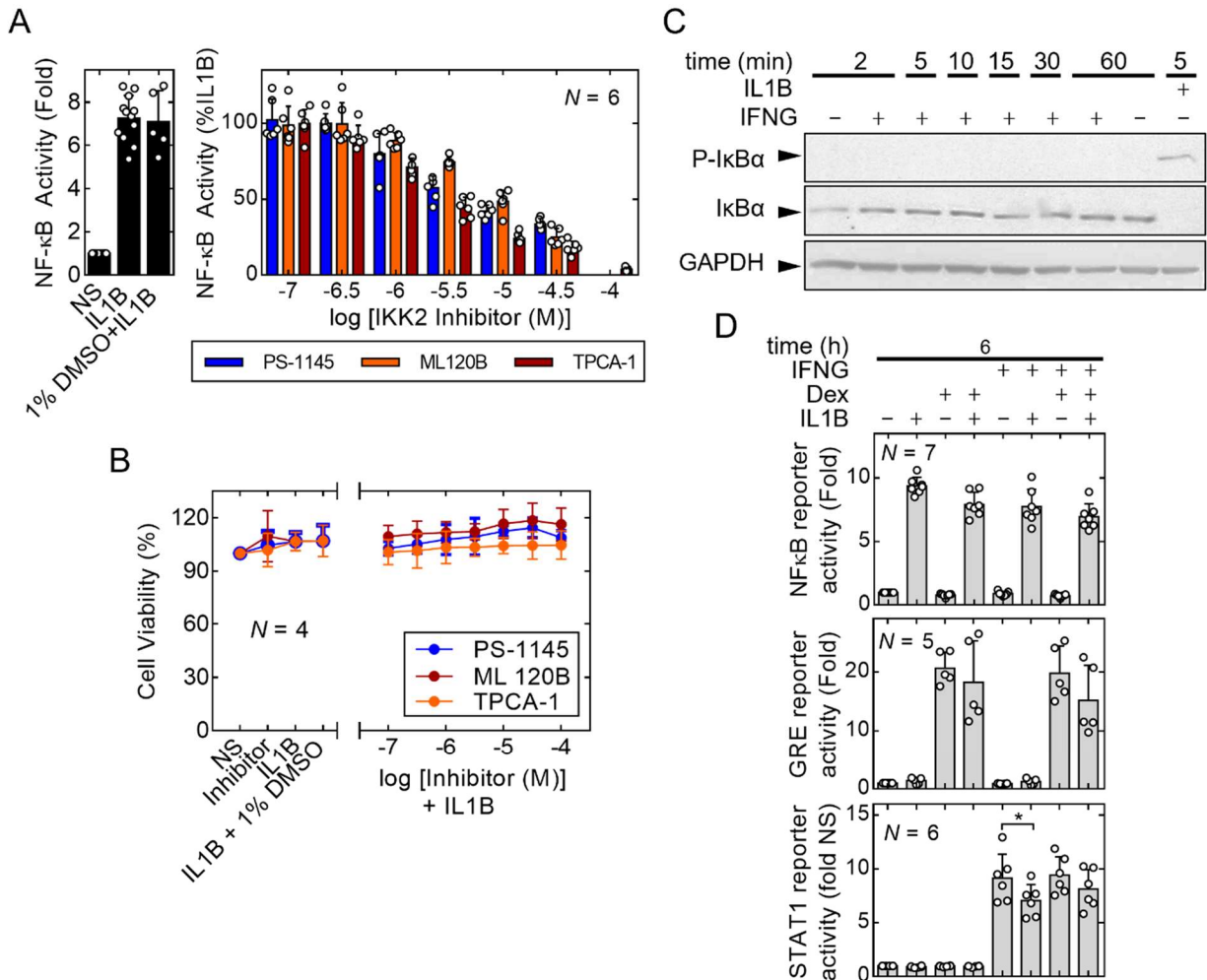
**Supplemental figure 1. Effect of IFNG, Dex or IL1B with each dual treatment on TLR2 expression in A549 cells.** Data for TLR2/GAPDH protein (A) or mRNA (B) were from figures 1, 2, 3, 4 & 8. A549 cells were treated with IL1B (1 ng/ml), dexamethasone (Dex, 1  $\mu$ M) and/or IFNG (10 ng/ml), as indicated. Cells were harvested at 24 h for western blot analysis or at 6 h for qPCR analysis of TLR2 and GAPDH. Data from *N* independent determinations were combined as TLR2 normalized to GAPDH. (Left panel) Consistent with being from separate experimental series with different investigators and, for protein, different antibodies, normality testing (D'Agostino & Pearson, Anderson-Darling, Shapiro-Wilk & Kolmogorov-Smirnov tests) suggested that data were not normally distributed. Individual data points are plotted with bars showing the median and 95% confidence intervals. Significance tested using ANOVA with a Tukey post-test is indicated where \*  $p \leq 0.05$ , \*\*  $p \leq 0.01$ , \*\*\*  $p \leq 0.001$ . Significance tested using a non-parametric ANOVA with a Dunn's post-test is indicated where #  $p \leq 0.05$ , ##  $p \leq 0.01$ , ###  $p \leq 0.001$ . (Right panels) To evaluate the consistency of the effect of adding each mono-treatment to the dual-treatments, data are shown as before and after plots, plus the effect difference (triple combination – dual treatment). Dashed lines indicate the mean of the dual treatment and triple treatment. Effect differentials for all data pairs are shown along with the mean and 95% confidence interval. Significance by paired t test (two tailed) is shown where \*  $p \leq 0.05$ , \*\*  $p \leq 0.01$ , \*\*\*  $p \leq 0.001$ . Significance by Wilcoxon matched-pairs signed rank test (two tailed) is shown where #  $p \leq 0.05$ , ##  $p \leq 0.01$ , ###  $p \leq 0.001$ .



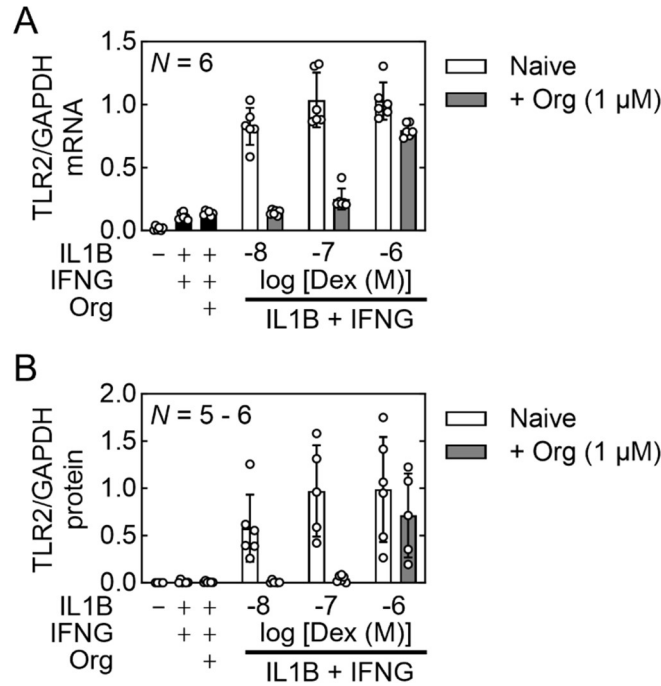
**Supplemental figure 2. Effect of IL1B, IFNG and budesonide on TLR2 expression in air-liquid interface primary human bronchial epithelial cells.** (A) pHBECs grown at air-liquid interface (ALI) were either not treated or treated with IL1B (1 ng/ml), IFNG (10 ng/ml) and/or budesonide (*Bud*; 300 nM), as indicated. Cells were harvested for western blot analysis of TLR2 and GAPDH at 6 and 24 h. Representative blots from *N* independent experiments are shown. (B) pHBECs grown as ALI cultures were treated as in A, prior to harvesting at 6 or 24 h for qPCR analysis of TLR2 and GAPDH mRNA. (*Upper graphs*) Data obtained from densitometry analysis (in A) and qPCR analysis (in B) were normalized to GAPDH, expressed as fold of untreated and mean  $\pm$  SD was plotted as bar graphs with overlaid scatter plots. Significance was tested using ANOVA with a Tukey post-hoc test. Asterisks (\*, \*\* or \*\*\*) represent significance relative to untreated. Hash (#, ##, ###) represent significance relative to IL1B + IFNG + Bud. (*Lower graphs*) The sum of each effect (i.e., fold - 1) within a group of treatments (*sum*) and the effect (fold - 1) for each combination treatment (*comb*) is expressed as mean  $\pm$  SD and plotted as bar graphs overlaid with scatter plots. Significance was tested using paired *t*-test. \*, #  $p \leq 0.05$ , \*\*, ##  $p \leq 0.01$ , \*\*\*, ###  $p \leq 0.001$ .



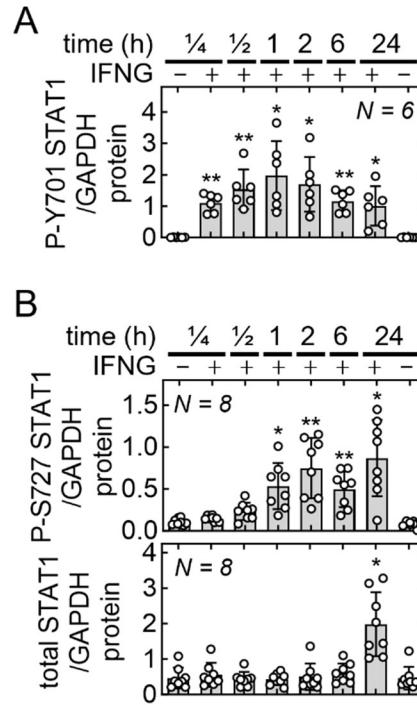
**Supplemental figure 3. Effect of IL1B, IFNG and glucocorticoids on GAPDH mRNA.** (A) A549 cells, or pHBECs grown in (B) submersion culture or (C) air-liquid interface (ALI) cultures, were either not treated, or treated with IL1B (1 ng/ml), IFNG (10 ng/ml) and/or dexamethasone (*Dex*; 1  $\mu$ M), as indicated. Cells were harvested at 6 or 24 h for qPCR analysis. In each case, mean  $C_t$  values of GAPDH from  $N$  independent experiments, are plotted as as bar graphs with overlaid scatter plots.



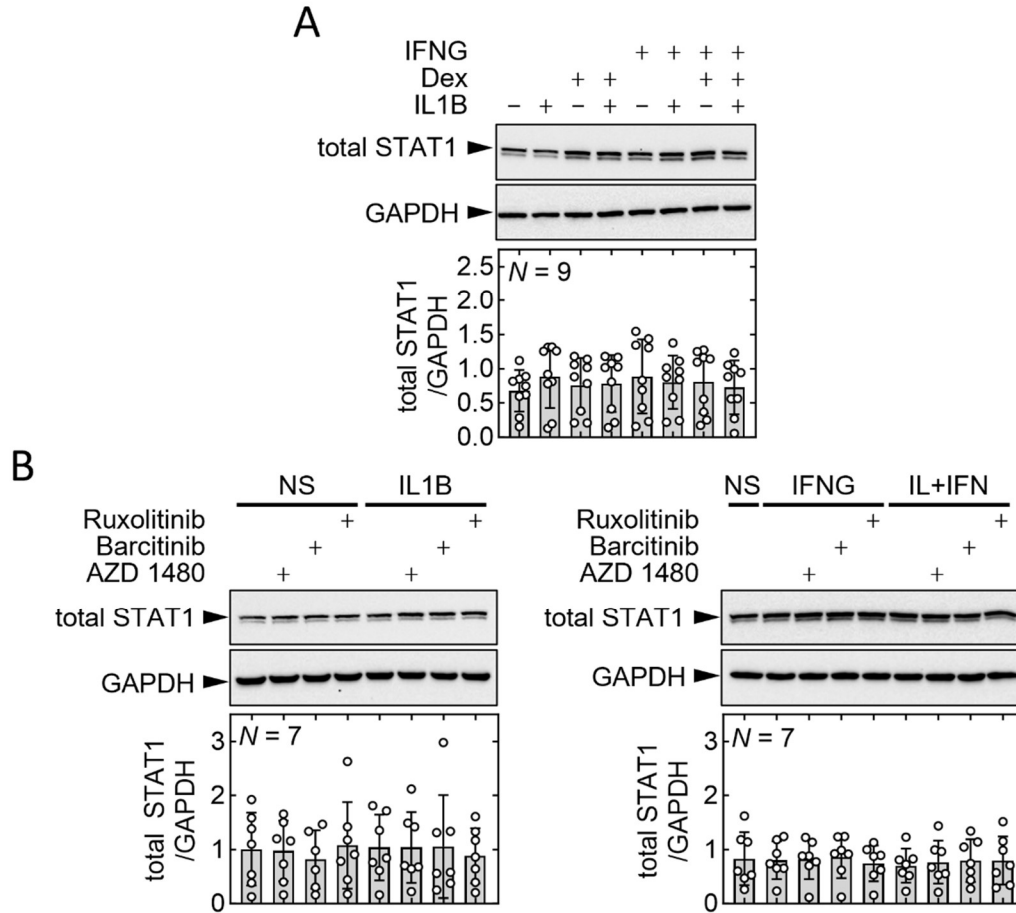
**Supplemental figure 4. NF- $\kappa$ B inhibition by IKK inhibitors and effects of IL1B, IFNG and Dex on NF- $\kappa$ B, GRE and STAT1 reporter activity.** A549 cells containing the NF- $\kappa$ B reporter, 6 $\kappa$ Btk.luc were either not treated, or pre-treated with 1% DMSO or indicated concentrations of PS-1145, ML120B or TPCA-1 for 90 min, prior to stimulation with IL1B (1 ng/ml). Cells were harvested for (A) luciferase assay and (B) MTT assay after 6 h. Data from  $N$  independent experiments was expressed as fold and % IL1B in A and as % cell viability in B, and plotted as mean (bars)  $\pm$  SD (error bars) overlaid with scatter plots. (C) A549 cells were treated with IFNG (10 ng/ml) for the indicated times prior to harvesting for western blot analysis of P-I $\kappa$ B $\alpha$ , I $\kappa$ B $\alpha$  and GAPDH. IL1B (1 ng/ml) was used as a positive control. Representative blots from 5 independent experiments are shown. (D) A549 cells containing the NF- $\kappa$ B reporter (6 $\kappa$ Btk.luc), GRE reporter (2 $\times$ GRE.luc) or STAT1 reporter (3 $\times$ STAT1.luc) were either not treated, or stimulated with IL1B (1 ng/ml), IFNG (10 ng/ml) and/or dexamethasone (*Dex*; 1  $\mu$ M) as indicated. Cells were harvested for luciferase assay at 6 h. Luciferase activity from  $N$  independent experiments was expressed as fold, and mean  $\pm$  SD was presented as bar graphs overlaid with scatter plots. Significance was tested using ANOVA with a Tukey post-hoc test. \*  $p \leq 0.05$ .



**Supplemental figure 5. Effect of Org 34517 on the enhancement of IL1B plus IFNG-induced TLR2 expression by dexamethasone.** (A) A549 cells were pretreated with Org 34517 (*Org*; 1  $\mu$ M) for 1 h, prior to stimulation with IL1B (1 ng/ml) plus IFNG (10 ng/ml) in absence or presence of various concentrations of dexamethasone (*Dex*). Cells were harvested for qPCR analysis at 6 h. TLR2 data, from  $N$  independent experiments, were normalized to GAPDH and means  $\pm$  SD were plotted as bar graphs overlaid with scatter plots. (B) Cells were treated as in A prior to harvesting for western blot analysis at 24 h. Densitometry data for TLR2 protein from  $N$  independent experiments were normalized to GAPDH (representative blots shown in Fig 4A) and means  $\pm$  SD were plotted as bar graphs overlaid with scatter plots.

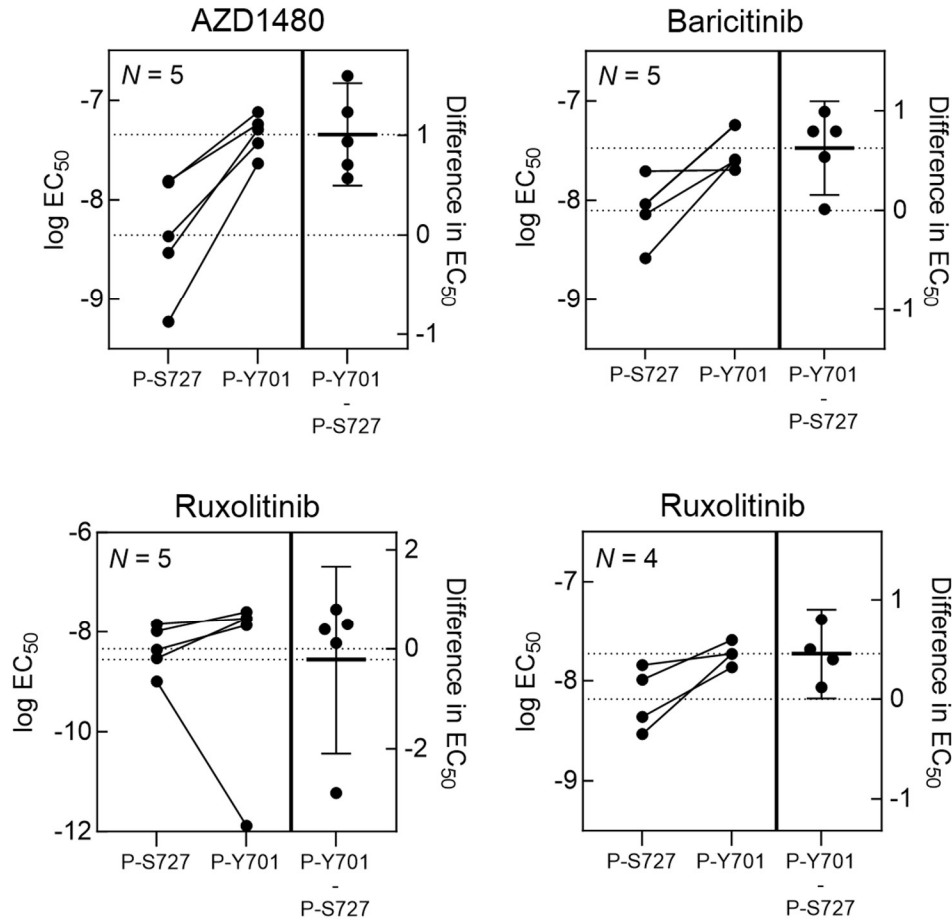


**Supplemental figure 6. Effect of IL1B, glucocorticoid and IFNG on STAT1 phosphorylation.** A549 cells were either untreated, or treated with IFNG (10 ng/ml), and harvested for western blot analysis at the indicated times. Representative blots from *N* independent experiments for P-STAT1 (Y701), P-STAT1 (S727), total STAT1 and GAPDH are shown in figure 5. Densitometric data for (A) P-STAT1 (Y701), and (B) P-STAT1 (S727) and total STAT1 were normalized to GAPDH and means  $\pm$  SD (error bars) were plotted as bar graphs overlaid with scatter plots. Significance relative to untreated at 1/4 h was assessed by ANOVA with a Dunnett's multiple comparison test.

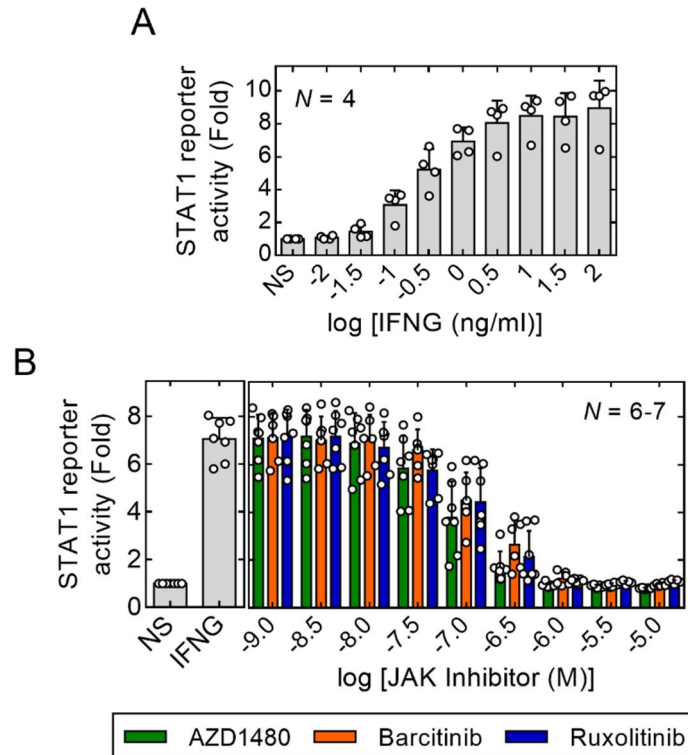


**Supplemental figure 7. Effect of IL1B, IFNG, Dex and JAK inhibitors on total STAT1 expression.** (A) A549 cells were either not treated, or stimulated with IL1B (1 ng/ml), IFNG (10 ng/ml) and/or dexamethasone (*Dex*; 1  $\mu$ M) as indicated. (B) A549 cells were either not stimulated or pre-treated with AZD1480, baricitinib or ruxolitinib, each at 1  $\mu$ M, for 1 h prior to stimulation with IL1B (1 ng/ml) and IFNG (10 ng/ml) as indicated. In each case, cells were harvested for western blot analysis. Representative blots of total STAT1 and GAPDH are shown. Densitometric data from *N* independent experiments were normalized to GAPDH and presented as mean  $\pm$  SD overlaid with scatter plots.

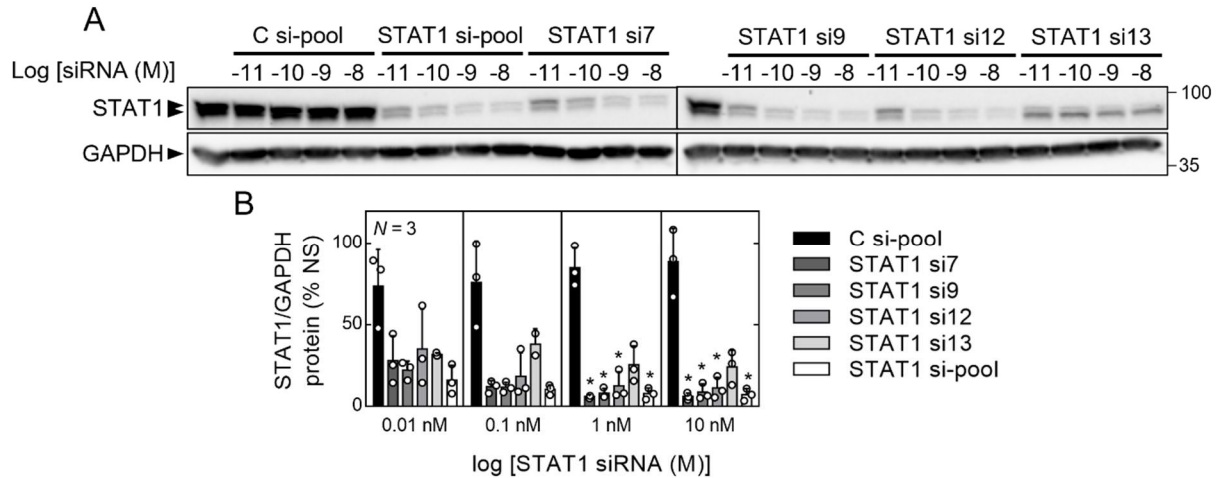




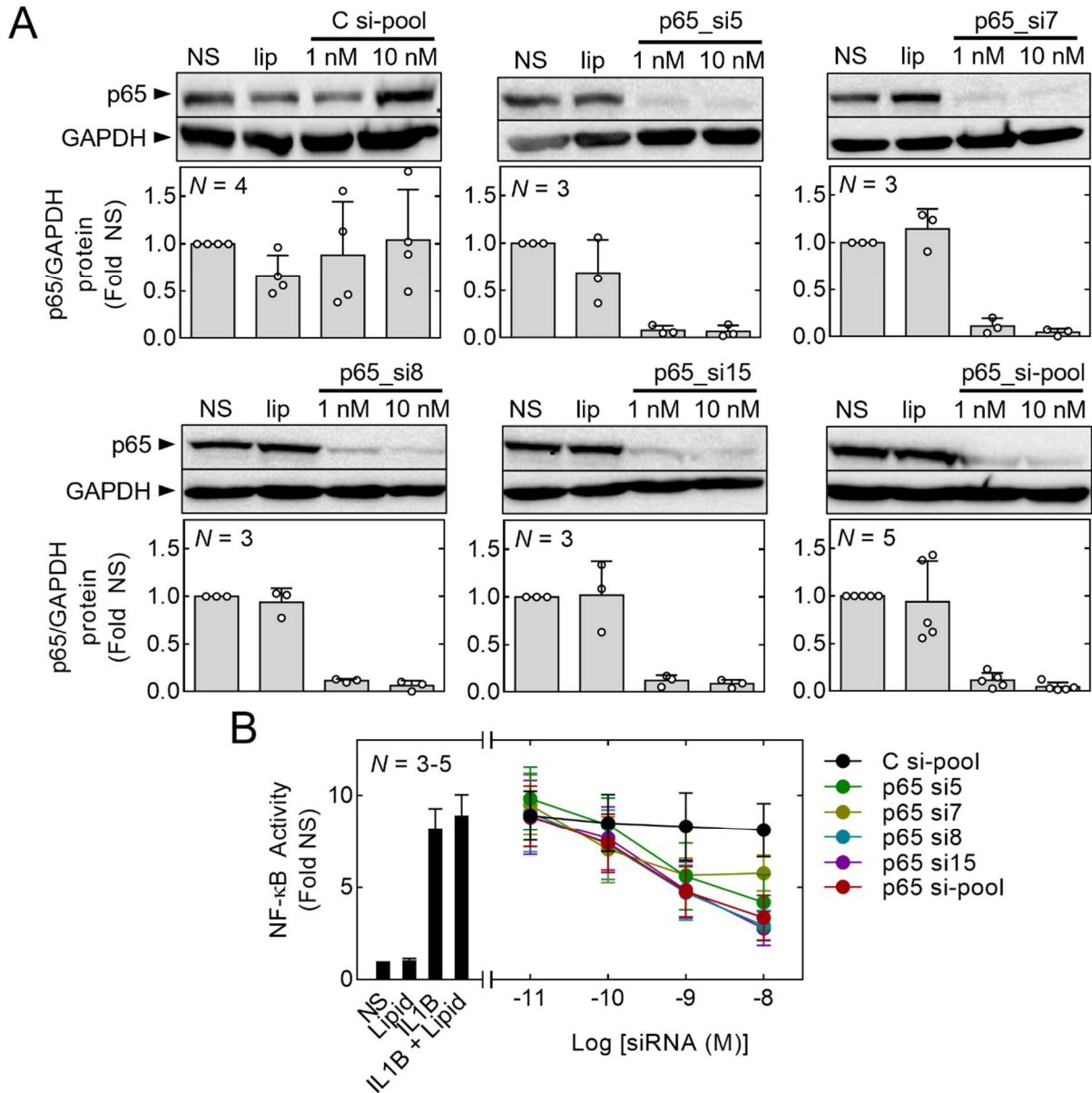
**Supplemental figure 8. EC<sub>50</sub> values for the effect of JAK inhibitors on STAT1 phosphorylation at Y701 and S727.** Data are from Fig. 6 of the main manuscript. A549 cells were pre-treated with AZD1480, baricitinib, and ruxolitinib at the indicated concentrations for 30 min, followed by stimulation with IFNG (10 ng/ml) for 1 h. Cells were harvested for western blot analysis of phospho-Y701 and S727 STAT1 and GAPDH. Densitometric data from the 5 experiments for Y701 P-STAT1 and S727 P-STAT1 were normalized to GAPDH. Data expressed as %IFNG effect for each of AZD1480, baricitinib, and ruxolitinib, were used to obtain paired log EC<sub>50</sub> values for each compound in respect of the inhibition of P-STAT1 (Y701) and P-STAT1 (S727) from each individual experiment. Paired log EC<sub>50</sub> values are shown as scatter plots (left side). For each pair the difference (PY701 – P727) in log EC<sub>50</sub> is also shown along with dotted lines to indicate the average log EC<sub>50</sub> for each group. For ruxolitinib, one dataset can be readily seen as having an outlier (lower left). The effect of excluding this data point is shown (lower right).



**Supplemental figure 9. Effect of IFNG and JAK inhibitors on STAT1 reporter activity.** (A) A549 cells stably transfected with 3×STAT1.luc luciferase reporter were either not stimulated (NS) or stimulated with the indicated concentrations of IFNG prior to harvesting for luciferase assay after 6 h. (B) A549. 3×STAT1.luc cells were either not stimulated (NS) or pre-treated with the indicated concentrations of AZD1480, barcitinib, or ruxolitinib for 30 mins followed by stimulation with IFNG (10 ng/ml). Cells were harvested for luciferase assay after 6 h. In each case, luciferase activity from *N* independent experiments was expressed as fold of NS and mean ± SD was plotted as bar graphs overlaid with scatter plots.



**Supplemental figure 10. Effect of STAT1 siRNAs on STAT1 expression.** (A) A549 cells were either not stimulated (*NS*), or incubated with the indicated concentrations of either control siRNA-pool (C si-pool), STAT1 siRNA-pool (STAT1 si-pool), or four individual STAT1 siRNAs (si7, si9, si12 and si13) for 48 h. Cells were then incubated overnight with serum-free media prior to harvesting for western blot analysis. Representative blots of STAT1 and GAPDH from *N* independent experiments are shown. (B) Data obtained from densitometry analysis were normalized to GAPDH and the percentage of *NS* is plotted as mean  $\pm$  SD overlaid with scatter plots. Significance relative to C si-pool at each siRNA concentration was tested using ANOVA with a Dunnett's post-hoc test. \*  $p \leq 0.05$ .



**Supplemental figure 11. Effect of p65 siRNAs on p65 expression and NF- $\kappa$ B activity. (A)** A549 cells were either not stimulated (NS), or incubated with the indicated concentrations of either control siRNA-pool (C si-pool), p65 siRNA-pool (STAT1 si-pool), or four individual p65 siRNAs (si5, si7, si8 and si15) for 48 h. Cells were then incubated overnight with serum-free media prior to harvesting for western blot analysis. Representative blots of STAT1 and GAPDH from *N* independent experiments are shown. Data obtained from densitometry analysis were normalized to GAPDH and the percentage of NS is plotted as mean  $\pm$  SD overlaid with scatter plots. **(B)** A549 cells containing the NF- $\kappa$ B reporter, 6 $\kappa$ Btk.luc were treated with the indicated concentrations of control siRNA-pool or p65 siRNAs as in A. Following overnight incubation with serum-free media, cells were either not stimulated (NS), or treated with IL1B for 6 h prior to harvesting for luciferase assay. Luciferase activity from *N* independent experiments was expressed as fold, and plotted as mean  $\pm$  SD.